Covariant mean-field calculations of finite-temperature nuclear matter

R. J. Furnstahl
Department of Physics and Astronomy, University of Maryland, College Park, Maryland 20742

Brian D. Serot*
Continuous Electron Beam Accelerator Facility, 12000 Jefferson Avenue, Newport News, Virginia 23606
and Physics Department and Nuclear Theory Center, Indiana University, Bloomington, Indiana 47405
(Received 24 July 1989)

Hot nuclear matter is studied in the framework of quantum hadrodynamics. General principles of covariant thermodynamics and thermodynamic consistency are discussed, and these principles are illustrated by computing nuclear matter properties in an arbitrary reference frame, using the mean-field approximation to the Walecka model. The results are shown to be Lorentz covariant, and thermodynamic consistency is demonstrated by proving the equality of the "thermodynamic" and "hydrostatic" pressures. The mean-field results are used in a simple hydrodynamic picture to discuss the phenomenology of heavy-ion collisions and astrophysical systems, with an emphasis on new features that arise in a covariant approach.

I. INTRODUCTION

The accurate description of hot, dense matter is an important problem in theoretical physics. Shortly after the Big Bang, the universe was composed entirely of hot, dense matter; calculations based on quantum field theory at finite temperature and density have been used to describe this pervasive quark-gluon plasma[1–4] and to investigate symmetry restoration.[5–8] In the present universe, the nuclear equation of state as a function of temperature, density, and the ratios of protons to neutrons and nucleons to hyperons is needed to study stellar collapse through a possible supernova phase into a neutron star.[9] On a smaller scale, we can explore the same nuclear dynamics through energetic collisions of heavy ions, where at least part of the hot matter can be described in terms of hadrons. Moreover, it is hoped that a quark-gluon plasma can be created in the laboratory at energies attainable in the proposed Relativistic Heavy-Ion Collider (RHIC), so that the transition between hadronic and subhadronic degrees of freedom can be studied.

To investigate this wide variety of phenomena, one needs a consistent microscopic treatment of strongly interacting, relativistic, quantum-mechanical systems. With such a framework we can compute both static thermodynamic properties (such as energy, pressure, and entropy) and dynamical characteristics (such as viscosity, transport coefficients, and collective modes and their damping). In addition, we can study the production and absorption of particles under extreme conditions and map out the nuclear matter phase diagram. Ultimately, we would like to develop techniques for nonequilibrium systems, in order to describe the development of two isolated nuclei into a single system in equilibrium.

In the nuclear domain, these problems are traditionally studied with the Schrödinger equation for nonrelativistic nucleons interacting through static, two-body potentials. Although the Schrödinger equation has been useful in this program for many years, new experimental facilities will force us to extend this framework to compare calculations with the data of the future. A more complete treatment of hadronic systems should include relativistic motion of the nucleons, dynamical mesons and baryon resonances, modifications of the nucleon structure in the nucleus, and the dynamics of the quantum vacuum, while maintaining general properties of quantum mechanics, covariance, gauge invariance, and causality. These physical effects will be relevant regardless of the degrees of freedom used to describe the system, and they must be studied simultaneously and consistently to draw definite conclusions about nuclear dynamics at high temperatures, high densities, and short distances.

In this paper, we study hot, dense nuclear matter using a renormalizable, relativistic quantum field theory of mesons and baryons, which is known as quantum hadrodynamics (QHD).[10] QHD is consistent in the sense that the dynamical assumptions (such as the relevant degrees of freedom, the form of the Lagrangian, and the normalization conditions) are made at the outset, and one then attempts to extract concrete results from the implied formalism. In principle, the assumptions permit the formulation of systematic, "conserving" approximations[11,12] that maintain the important general properties mentioned earlier. Calculations can then be compared to data to see if the framework is related to the real world, and to decide where QHD succeeds and where it fails.

We focus on some general aspects of relativistic many-body systems at finite temperature and density, such as covariant formulations of thermodynamics and the preservation of thermodynamic consistency in microscopic calculations. We illustrate these aspects by performing a covariant calculation of finite-temperature nuclear matter properties in the mean-field approximation

to the Walecka model (QHD-I).[13,10] This model contains some basic elements of hadronic theories of nuclei, namely, baryons coupled strongly to neutral scalar and vector fields. Although this is a simple calculation, it produces some informative results, such as the Lorentz transformation properties of the temperature and chemical potential; it also illustrates that a preferred frame (the frame of the "thermal bath" in contact with our system) does not destroy the covariance. In a future paper, we will describe systematic techniques for going beyond the mean-field approximation using covariant, finite-temperature Feynman rules in real and imaginary time. These techniques are based on a path-integral representation of the quantum partition function extended to the complex time plane[14] and can be used to compute both static thermodynamic properties and dynamical characteristics. The calculations presented here provide a convenient benchmark for our discussion of more general techniques, and also introduce concepts that will be important in subsequent developments.

There are several reasons for considering models with only hadronic degrees of freedom. First, these variables are the most efficient at low densities and temperatures and for describing particle emission and absorption, as hadrons are the particles observed experimentally. Second, hadronic calculations can be calibrated by comparing to observed hadron-hadron scattering and empirical nuclear properties; we can then extrapolate to extreme conditions and test the predictions of the models. Third, the formulation of practical, reliable techniques for finite-density calculations in strong-coupling relativistic quantum field theories is a problem that is basically unsolved.[15–17] The development of such tools in a hadronic field theory is not only useful in its own right, but it may also provide insight into similar approaches for quantum chromodynamics (QCD). Finally and most importantly, we must understand the limitations of a purely hadronic theory to deduce true signals of QCD behavior in nuclear matter.

We consider three main topics in the present work. First, we discuss thermodynamic consistency in calculations of hot, dense nuclear matter. Consistency implies that the "thermodynamic" pressure calculated from the thermodynamic potential agrees with the "hydrostatic" pressure computed from the trace of the stress tensor. (This is sometimes called the virial theorem.[14]) The mean-field theory is consistent (as we demonstrate), as is the exact quantum field theory,[14] but it is difficult to obtain consistency in other approximations to the relativistic many-body problem.[18] This is an important topic for future work. We also study how covariance is achieved by comparing a canonical calculation carried out directly in a frame where the nuclear matter is moving to one performed in the frame where the matter is at rest. Although manifest covariance disappears in the calculation, we show that the results are covariant and relate them to a manifestly covariant formulation. Finally, we illustrate our covariant results using hydrodynamic models to describe the systematics of heavy-ion collisions and astrophysical systems. Although the hydrodynamic approach in infinite matter is an oversimplification, it gives the most direct connection to the thermodynamics and allows us to study new ideas in a simple fashion. In particular, the covariant approach elevates the velocity and momentum density of the system to the status of conjugate thermodynamic parameters, and we examine the implications for dense, rapidly flowing systems. We postpone to a future paper the extension of these results to more sophisticated approximations.

The outline of this paper is as follows: In Sec. II, we discuss covariant thermodynamics, establish notation, and present working definitions of Lorentz covariance and thermodynamic consistency. In Sec. III, hot, flowing nuclear matter is studied in the mean-field approximation to the Walecka model, using the familiar procedures of canonical quantization. In Sec. IV, we examine the properties of nuclear matter, concentrating on the differences that arise when the matter is observed in uniform motion. We also examine the nuclear matter phase diagram and the various regions of phase space that may be achieved in current heavy-ion experiments. We emphasize, however, that our results are obtained from a simple approximation to a simple model; our focus is not on quantitatively accurate predictions but rather on basic and important features of hot, dense, relativistic many-body systems. Many of these features will remain in more sophisticated calculations.

II. COVARIANT THERMODYNAMICS

Here we summarize some important formulas for the covariant description of a uniform, isolated system in equilibrium. These results are not new; our purpose is to define notation, to establish working definitions of Lorentz covariance and thermodynamic consistency, and to clarify which calculated quantities provide nontrivial tests of the consistency of a particular approximation. For a more complete discussion of the thermodynamic formalism, see Refs. 2, 19, and 20.

We begin by defining *primary thermodynamic functions* for the equilibrium system:

$$\text{energy-momentum tensor: } T^{\mu\nu} , \tag{2.1}$$

$$\text{entropy flux vector: } S^{\mu} , \tag{2.2}$$

$$\text{baryon current density vector: } B^{\mu} . \tag{2.3}$$

These quantities are covariant and involve no specification of a particular reference frame. We assume the conservation laws

$$\partial_{\mu} T^{\mu\nu}=0, \quad \partial_{\mu} B^{\mu}=0 , \tag{2.4}$$

and the symmetry of $T^{\mu\nu}$. Our conventions are those of Ref. 10, with a metric $g^{\mu\nu}=\text{diag}(+,-,-,-)$, and we use natural units with $\hbar=c=k_{\text{B}}=1$.

Our main objective is to compute these thermodynamic functions by taking ensemble averages of the corresponding quantum-mechanical operators, which will be denoted with carets, for example, $\hat{T}^{\mu\nu}$. In the theories we consider, the conservation laws (2.4) are satisfied as a consequence of the field equations resulting from the model Lagrangian. Moreover, although it is possible to

construct a symmetric energy-momentum-tensor operator $\hat{T}^{\mu\nu}=\hat{T}^{\nu\mu}$, this is unnecessary for a uniform system. (The nonsymmetric part of $\hat{T}^{\mu\nu}$ can be written as a total divergence, whose diagonal matrix elements vanish between eigenstates of total four-momentum.[21])

The primary thermodynamic quantities (2.1)–(2.3) are generally functions of six variables:

$$\text{baryon thermal potential: } \alpha \ , \tag{2.5}$$

$$\text{inverse temperature: } \beta \ , \tag{2.6}$$

$$\text{fluid four-velocity: } u^{\mu} \ , \tag{2.7}$$

$$\text{volume: } V \ . \tag{2.8}$$

The volume V will be taken large and *fixed* throughout the calculation; we let $V\rightarrow\infty$ at the end to define the "thermodynamic limit" and restore invariance under translations. The quantities α and β are Lorentz scalars defined by

$$\beta\equiv\frac{1}{T'}, \quad \alpha\equiv\frac{\mu'}{T'} \ , \tag{2.9}$$

where T' and μ' are the temperature and baryon chemical potential in the comoving frame, where the fluid three-velocity $\mathbf{v}=0$. Throughout this work, when we refer to a quantity that may be defined by an observer in any frame, the value taken in the comoving frame will be denoted with a prime. The primed value is, by definition, a Lorentz scalar, and these scalars are commonly used as the thermodynamic variables for the system.[20,22,2] For the present development, however, it will be more convenient to allow all observers to define their own temperature, chemical potential, etc., and a prime simply distinguishes the value observed in the comoving frame.

The fluid four-velocity vector u^{μ} can be written in terms of the three-velocity $\mathbf{v}$ as

$$u^{\mu}=\eta(1,\mathbf{v}), \quad \eta\equiv(1-\mathbf{v}^2)^{-1/2} \ . \tag{2.10}$$

(We reserve the more conventional symbol γ for later use.) There are only three independent components in u^{μ}, since $u_{\mu}u^{\mu}=1$. In the comoving frame, $u^{\mu'}=(1,0)$. It is also convenient to introduce a timelike thermal four-vector

$$\beta^{\mu}\equiv\beta u^{\mu}\equiv\frac{1}{T'}u^{\mu} \ , \tag{2.11}$$

which depends on the four independent variables β and $\mathbf{v}$.

One now introduces *secondary thermodynamic functions* that are defined in the comoving frame and are thus Lorentz scalars:

$$\text{pressure: } p'=p \ , \tag{2.12}$$

$$\text{proper energy density: } \mathcal{E}' \ , \tag{2.13}$$

$$\text{proper entropy density: } \sigma' \ , \tag{2.14}$$

$$\text{proper baryon density: } \rho'_{\mathrm{B}} \ , \tag{2.15}$$

$$\text{scalar density: } \rho'_{\mathrm{s}}=\rho_{\mathrm{s}} \ . \tag{2.16}$$

The pressure p and the scalar density of baryons ρ_{s} are the same in all frames,[19] so the primes are superfluous. In the thermodynamic limit, these secondary quantities are functions of α and β (or μ' and T') only.

The secondary thermodynamic functions can be used to construct the primary functions in any frame:

$$T^{\mu\nu}=(\mathcal{E}'+p)u^{\mu}u^{\nu}-pg^{\mu\nu} \ , \tag{2.17}$$

$$S^{\mu}=\sigma' u^{\mu} \ , \tag{2.18}$$

$$B^{\mu}=\rho'_{\mathrm{B}}u^{\mu} \ . \tag{2.19}$$

In the thermodynamic limit, the primary quantities are functions of α, β, and u^{μ}, or equivalently, α and β^{μ}. We now make the following working definition.

If the theory (or approximation) is Lorentz covariant, calculation of the secondary quantities and insertion into Eqs. (2.17)–(2.19) should give the same result as the direct evaluation of the primary quantities (2.1)–(2.3) in a frame where $\mathbf{v}\neq 0$.

There has recently been some controversy[23,24] regarding Lorentz covariance in calculations of relativistic many-body systems. Difficulties may arise when one tries to construct approximations to boost operators or states. Nevertheless, the covariant calculation of *matrix elements* (thermodynamic functions, Green's functions, S-matrix elements, etc.) is straightforward in a uniform system, even at finite temperature and density.[25] In the next section, we demonstrate how covariant matrix elements can be calculated in a canonical approach.

With the preceding definitions, we can discuss the thermodynamics of the system. All equilibrium results follow from the first law of thermodynamics, which is written covariantly as[20]

$$\beta_{\nu}dT^{\nu\mu}=dS^{\mu}+\alpha\, dB^{\mu} \ . \tag{2.20}$$

This important expression can be recast in more familiar form by inserting Eqs. (2.17)–(2.19). After taking the indicated differentials and realizing that u^{μ} and du^{μ} are orthogonal vectors, we find the two scalar equations

$$d\mathcal{E}'=T'd\sigma'+\mu' d\rho'_{\mathrm{B}} \ , \tag{2.21}$$

$$\mathcal{E}'=-p+T'\sigma'+\mu'\rho'_{\mathrm{B}} \ . \tag{2.22}$$

These will be recognized as the usual first law and Gibbs' relation,[26] written in the comoving frame at fixed volume V'. Equation (2.21) produces the familiar thermodynamic results at fixed volume

$$\left[\frac{\partial\mathcal{E}'}{\partial\sigma'}\right]_{V',\rho'_{\mathrm{B}}}=T', \quad \left[\frac{\partial\mathcal{E}'}{\partial\rho'_{\mathrm{B}}}\right]_{V',\sigma'}=\mu' \ . \tag{2.23}$$

Moreover, if we specialize to a system at zero temperature, a combination of Eqs. (2.22) and (2.23) reveals

$$p=(\rho'_{\mathrm{B}})^2\frac{\partial}{\partial\rho'_{\mathrm{B}}}\left[\frac{\mathcal{E}'}{\rho'_{\mathrm{B}}}\right] \quad (T=0) \ . \tag{2.24}$$

These results allow us to make another working definition.

If the theory (or approximation) is thermodynamically consistent, secondary quantities calculated from operator ensemble averages should satisfy Gibbs' relation and the corresponding differential laws.

This definition of consistency is most important when applied to the pressure, since p can be computed from either the thermodynamic potential[26] or from the trace of the stress tensor.[27] (See the discussion below.) We will call an approximation thermodynamically consistent only if the two results for the pressure agree.

If we rewrite Eq. (2.22) as

$$\begin{aligned} pu^\mu &= -\mathcal{E}'u^\mu + T'\sigma' u^\mu + \mu'\rho'_{\rm B}u^\mu \\ &= -u_\nu T^{\nu\mu} + T'S^\mu + \mu' B^\mu , \end{aligned} \tag{2.25}$$

division by T' gives the covariant form of Gibbs' relation

$$p\beta^\mu = -\beta_\nu T^{\nu\mu} + S^\mu + \alpha B^\mu . \tag{2.26}$$

This expression can be rewritten as a differential relation using Eq. (2.20), with the result

$$d(p\beta^\mu) = -T^{\nu\mu}d\beta_\nu + B^\mu d\alpha . \tag{2.27}$$

If a calculation is both Lorentz covariant and thermodynamically consistent (as defined above), then both (2.26) and (2.27) should hold. Since the (constant volume) thermodynamic functions depend only on α and β^μ, Eq. (2.27) implies

$$\left[\frac{\partial(p\beta^\mu)}{\partial\beta_\nu}\right]_\alpha = -T^{\nu\mu}, \quad \left[\frac{\partial(p\beta^\mu)}{\partial\alpha}\right]_{\beta_\nu} = B^\mu . \tag{2.28}$$

Note that these manipulations require greater care for systems at zero temperature. In particular, one must return to Eq. (2.25) and remember that u^μ has only three independent components to derive

$$d(pu^\mu) = (v^i T^{0\mu} - T^{i\mu})du_i + B^\mu d\mu' \quad (T=0) . \tag{2.29}$$

To compute the thermodynamic functions in a particular theory, one must relate them to ensemble averages of quantum-mechanical operators. This is achieved by defining a *grand partition function* Z and a four-vector thermodynamic potential $\Phi^\mu = \Phi^\mu(\alpha,\beta^\nu)$ through

$$\begin{aligned} Z &\equiv \exp\left[-\int d\Lambda_\mu \Phi^\mu(\alpha,\beta^\nu)\right] \\ &\equiv \mathrm{Tr}\left[\exp\left[-\int d\Lambda_\mu(\beta_\nu \hat{T}^{\nu\mu} - \alpha\hat{B}^\mu)\right]\right] . \end{aligned} \tag{2.30}$$

Here Λ_μ is a spacelike hypersurface, and these expressions are manifestly Lorentz invariant. In the comoving frame, Eq. (2.30) reduces to the familiar result

$$Z = \mathrm{Tr}\{\exp[-\beta(\hat{H} - \mu'\hat{B})]\} , \tag{2.31}$$

where $\hat{H}$ is the Hamiltonian and $\hat{B}$ is the baryon number operator. The motivation and justification for Eq. (2.30) will be discussed in Sec. III, where we show how this definition arises naturally from a canonical calculation of the grand partition function in an arbitrary reference frame.

If one makes small variations in β^μ and α, it follows immediately from Eq. (2.30) that

$$d\Phi^\mu = T^{\mu\nu}d\beta_\nu - B^\mu d\alpha . \tag{2.32}$$

Here the classical quantities on the right-hand side are defined as usual by ensemble averages:

$$\begin{aligned} A &\equiv \langle\langle \hat{A} \rangle\rangle \\ &= Z^{-1}\mathrm{Tr}\left[\hat{A}\exp\left[-\int d\Lambda_\mu(\beta_\nu\hat{T}^{\nu\mu} - \alpha\hat{B}^\mu)\right]\right] . \end{aligned} \tag{2.33}$$

Thus we have

$$\left[\frac{\partial\Phi^\mu}{\partial\beta_\nu}\right]_\alpha = T^{\mu\nu}, \quad \left[\frac{\partial\Phi^\mu}{\partial\alpha}\right]_{\beta_\nu} = -B^\mu . \tag{2.34}$$

To relate the thermodynamic four-potential Φ^μ to more familiar quantities, recall that the conventional thermodynamic potential[26]

$$\Omega \equiv \Omega(T',V',\mu') = (\mathcal{E}' - T'\sigma' - \mu'\rho'_{\rm B})V' \tag{2.35}$$

in the comoving frame can be used to define the "thermodynamic pressure"

$$p \equiv \frac{-\Omega(T',V',\mu')}{V'} . \tag{2.36}$$

A comparison of Eqs. (2.28) and (2.34) implies that

$$\begin{aligned} \Phi^\mu(\alpha,\beta^\nu) &= -p\beta^\mu = \frac{\Omega(T',V',\mu')}{V'}\beta^\mu \\ &= \frac{\Omega(T',V',\mu')}{V'T'}u^\mu , \end{aligned} \tag{2.37}$$

so that

$$\Phi^\mu = \beta_\nu T^{\nu\mu} - S^\mu - \alpha B^\mu . \tag{2.38}$$

If a calculation is Lorentz covariant, the computation of Φ^μ from Eq. (2.37) should agree with the result determined directly from (2.30) in an arbitrary frame. If the calculation is also thermodynamically consistent, the thermodynamic pressure determined from Eq. (2.36) or (2.37) should agree with the "hydrostatic" pressure defined by the ensemble average of the stress-tensor operator in the comoving frame:

$$p = \tfrac{1}{3}\langle\langle \hat{T}'_{i'i'} \rangle\rangle . \tag{2.39}$$

This equality of the thermodynamic and hydrostatic pressures is sometimes called the virial theorem,[14] because the classical virial theorem of Clausius is implied by it. Whereas the theorem holds as an exact result in relativistic quantum field theory, it is often difficult to maintain in approximate calculations.[18]

III. HOT, FLOWING NUCLEAR MATTER

To illustrate the ideas in the preceding section and to provide a concrete example of a covariant calculation, we consider a uniform system of hot, flowing nuclear matter. We work in the mean-field approximation to the Walecka model,[13,10] in which Dirac nucleons interact with classical scalar and vector fields. Vacuum contributions will be ignored here for simplicity, but can be included straightforwardly in this renormalizable model.[21,25]

Hot nuclear matter[21,28,10] and flowing nuclear matter[29,30,10] have been studied separately in this model, but to our knowledge, the present calculation is the first to treat the general case.[31] Extensions beyond the mean-field approximation are postponed to a forthcoming pa-

per,[25] where we derive covariant Feynman rules for systems described by quantum hadrodynamics at finite temperature and density.

We have three goals in this section. First, we want to illustrate the calculation of thermodynamic functions in an arbitrary reference frame. By relating the results to those computed in the comoving frame, the covariance of the calculation can be verified. Second, we want to discuss the thermodynamic constraints, showing which are satisfied trivially and which are not. Third, we want to justify the covariant definition of the partition function in Eq. (2.30). Clearly, if one *starts* with this definition, the resulting calculation of the trace is guaranteed to be covariant. In contrast, our approach begins with a straightforward canonical treatment of the thermodynamics of a moving relativistic fluid. Although manifest Lorentz covariance is lost, we prove that the calculated results are covariant and then show that the canonical partition function agrees with Eq. (2.30) for a particular choice of hypersurface Λ_μ. In Sec. IV, we discuss some of the physical properties of hot, flowing nuclear matter in this simple relativistic model.

Our starting point is the mean-field theory (MFT) Lagrangian for the Walecka model. (This is called QHD-I in Ref. 10.) Since the nuclear medium is homogeneous, the classical meson fields ϕ and V^μ are constant, but since the matter is flowing with velocity $\mathbf{v}$, there is a uniform baryon flux $\mathcal{B}$. Thus the classical vector field has both temporal and spatial components: $V^\mu=(V_0,\mathbf{V})$, and the mean-field Lagrangian density is

$$\mathcal{L}_{\rm MFT}=\bar\psi[\gamma_\mu(i\partial^\mu-g_{\rm v}V^\mu)-(M-g_{\rm s}\phi)]\psi -\tfrac{1}{2}m_{\rm s}^2\phi^2+\tfrac{1}{2}m_{\rm v}^2V^\mu V_\mu \ . \tag{3.1}$$

The conserved baryon four-current and energy-momentum tensor can be derived in the usual fashion,[32,33] resulting in

$$B^\mu\equiv(\rho_{\rm B},\mathcal{B})=\bar\psi\gamma^\mu\psi \ , \tag{3.2}$$

$$T^{\mu\nu}=i\bar\psi\gamma^\mu\partial^\nu\psi-\tfrac{1}{2}(m_{\rm v}^2V^\lambda V_\lambda-m_{\rm s}^2\phi^2)g^{\mu\nu} \ . \tag{3.3}$$

Since the meson fields are classical, only the fermion field must be quantized. The Dirac field equation follows from $\mathcal{L}_{\rm MFT}$,

$$[i\gamma_\mu\partial^\mu-g_{\rm v}\gamma_\mu V^\mu-(M-g_{\rm s}\phi)]\psi(t,\mathbf{x})=0 \ , \tag{3.4}$$

and since this equation is linear, it can be solved exactly. We look for normal-mode solutions of the form

$$\begin{aligned}\psi_{\mathbf{k}\lambda}^{(+)}(t,\mathbf{x})&=U(\mathbf{k},\lambda)e^{i\mathbf{k}\cdot\mathbf{x}-i\epsilon^{(+)}(\mathbf{k})t} \ ,\\ \psi_{\mathbf{k}\lambda}^{(-)}(t,\mathbf{x})&=V(\mathbf{k},\lambda)e^{-i\mathbf{k}\cdot\mathbf{x}-i\epsilon^{(-)}(-\mathbf{k})t} \ ,\end{aligned} \tag{3.5}$$

so that the spinors obey

$$\begin{aligned}&[\epsilon^{(+)}(\mathbf{k})-g_{\rm v}V_0]U(\mathbf{k},\lambda)=[\boldsymbol{\alpha}\cdot(\mathbf{k}-g_{\rm v}\mathbf{V})+\beta M^*]U(\mathbf{k},\lambda) \ ,\\ &[\epsilon^{(-)}(-\mathbf{k})-g_{\rm v}V_0]V(\mathbf{k},\lambda)\\ &\qquad=[\boldsymbol{\alpha}\cdot(-\mathbf{k}-g_{\rm v}\mathbf{V})+\beta M^*]V(\mathbf{k},\lambda) \ ,\end{aligned} \tag{3.6}$$

where $M^*\equiv M-g_{\rm s}\phi$. (The Dirac matrices $\boldsymbol{\alpha}$ and β should not be confused with the thermodynamic parameters introduced in Sec. II.) These conventions are useful, since the resulting single-particle spectrum can be written in the compact form

$$\begin{aligned}\epsilon^{(\pm)}(\mathbf{k})&=g_{\rm v}V_0\pm[(\mathbf{k}-g_{\rm v}\mathbf{V})^2+M^{*2}]^{1/2}\\ &\equiv g_{\rm v}V_0\pm(\boldsymbol{\kappa}^2+M^{*2})^{1/2}\\ &\equiv g_{\rm v}V_0\pm E^*(\boldsymbol{\kappa}) \ ,\end{aligned} \tag{3.7}$$

where the second line defines the *kinetic momentum* $\boldsymbol{\kappa}\equiv\mathbf{k}-g_{\rm v}\mathbf{V}$, and the final line defines $E^*(\boldsymbol{\kappa})$.

The baryon field operator can be written as

$$\psi(t,\mathbf{x})=V^{-1/2}\sum_{\mathbf{k}\lambda}[\,A_{\mathbf{k}\lambda}U(\mathbf{k},\lambda)e^{i\mathbf{k}\cdot\mathbf{x}-i\epsilon^{(+)}(\mathbf{k})t} +B_{\mathbf{k}\lambda}^\dagger V(\mathbf{k},\lambda)e^{-i\mathbf{k}\cdot\mathbf{x}-i\epsilon^{(-)}(-\mathbf{k})t}] \ , \tag{3.8}$$

where V is the volume of the system and the spinors have the (noncovariant) normalization

$$U^\dagger(\mathbf{k},\lambda)U(\mathbf{k},\lambda')=V^\dagger(\mathbf{k},\lambda)V(\mathbf{k},\lambda')=\delta_{\lambda\lambda'} \ .$$

We now impose the equal-time anticommutation relations

$$\begin{aligned}&\{\psi(t,\mathbf{x}),\psi^\dagger(t,\mathbf{y})\}=\delta^{(3)}(\mathbf{x}-\mathbf{y}) \ ,\\ &\{\psi(t,\mathbf{x}),\psi(t,\mathbf{y})\}=\{\psi^\dagger(t,\mathbf{x}),\psi^\dagger(t,\mathbf{y})\}=0 \ ,\end{aligned} \tag{3.9}$$

which produce the familiar anticommutators for the mode amplitudes $A_{\mathbf{k}\lambda}$, $A_{\mathbf{k}\lambda}^\dagger$, $B_{\mathbf{k}\lambda}$, and $B_{\mathbf{k}\lambda}^\dagger$.

The field operators ψ and $\psi^\dagger$ can now be used to construct the baryon number operator $\hat B\equiv\int d^3x\,\bar\psi\gamma^0\psi$ and the four-momentum operators $\hat P^\mu=(\hat H,\hat{\mathbf{P}})\equiv\int d^3x\,T^{0\mu}$, with the results[34]

$$\hat B=\sum_{\mathbf{k}\lambda}(A_{\mathbf{k}\lambda}^\dagger A_{\mathbf{k}\lambda}-B_{\mathbf{k}\lambda}^\dagger B_{\mathbf{k}\lambda}) \ , \tag{3.10}$$

$$\hat H=\sum_{\mathbf{k}\lambda}E^*(\boldsymbol{\kappa})(A_{\mathbf{k}\lambda}^\dagger A_{\mathbf{k}\lambda}+B_{-\mathbf{k}\lambda}^\dagger B_{-\mathbf{k}\lambda})+g_{\rm v}V_0\hat B +\tfrac{1}{2}(m_{\rm s}^2\phi^2+m_{\rm v}^2\mathbf{V}^2-m_{\rm v}^2V_0^2)V \ , \tag{3.11}$$

$$\hat{\mathbf{P}}=\sum_{\mathbf{k}\lambda}\mathbf{k}(A_{\mathbf{k}\lambda}^\dagger A_{\mathbf{k}\lambda}+B_{\mathbf{k}\lambda}^\dagger B_{\mathbf{k}\lambda}) \ . \tag{3.12}$$

Note that $\hat{\mathbf{P}}$ involves a sum over canonical momenta $\mathbf{k}$, not kinetic momenta $\boldsymbol{\kappa}$. To obtain these expressions, the operator products have been *normal ordered*, so that all destruction operators are to the right, and c-number pieces have been omitted. As discussed in Ref. 10, the c-number contribution to the Hamiltonian leads to vacuum corrections, which we will neglect here. Note that, in principle, there are also contributions to the energy and momentum from thermal excitation of real mesons. Since these do not become appreciable (in this model) until very high temperatures ($T\gtrsim m_{\rm s}$, $m_{\rm v}$), we omit these terms.

The MFT Hamiltonian (3.11) is diagonal, so we have solved this model problem exactly (once we have specified the meson fields). Since $\hat B$ and $\hat{\mathbf{P}}$ are also diagonal, the baryon number and total momentum are constants of the motion, as are their corresponding densities $\rho_{\rm B}$ and $\mathcal{P}$, since the volume is fixed. At zero temperature, the

ground state of the moving medium is obtained[10,30] by filling energy levels up to a nonspherical Fermi surface $\mathbf{k}_F$. The shape of the Fermi surface is determined *thermodynamically* by minimizing the mean-field energy density $\mathcal{E}$ at fixed baryon density ρ_B and momentum density $\mathcal{P}$. This is achieved by introducing Lagrange multipliers for the chemical potential and flow velocity, so that the quantity to be minimized is

$$\mathcal{E}(\mathbf{k}_F;\phi,V_0,\mathbf{V})-\mu\rho_B(\mathbf{k}_F)-\mathbf{v}\cdot\mathcal{P}(\mathbf{k}_F) . \tag{3.13}$$

Note that the thermodynamic quantities appearing in this expression are defined in the "laboratory" frame, where the fluid has velocity $\mathbf{v}$.

To describe the system at finite temperature, we need a thermodynamic potential and partition function that will select the correct ground state in the $T\to 0$ limit. Thus we are naturally led to define

$$\begin{aligned} Z &= \mathrm{Tr}\exp[-(\hat{H}-\mu\hat{B}-\mathbf{v}\cdot\hat{\mathbf{P}})/T] \\ &\equiv \exp[-\Omega(T,V,\mu,\mathbf{v})/T] . \end{aligned} \tag{3.14}$$

As before, all thermodynamic parameters in this expression are defined by an observer in the laboratory frame. In addition, as is clear from the discussion before Eqs. (3.10)–(3.12), the thermodynamic functions $\mathcal{E}$, ρ_B, and $\mathcal{P}$ are defined in a natural way for this observer. The relation of these observables to those in the comoving frame (the "primed" observables), as well as the connection between Eqs. (3.14) and (2.30) will be clarified in the subsequent discussion. The thermodynamic potential Ω also depends parametrically on the meson fields, which will be chosen to make Ω stationary.

The first law of thermodynamics in the laboratory frame reads

$$dE = T\,dS - p\,dV + \mu\,dB + \mathbf{v}\cdot d\mathbf{P} , \tag{3.15}$$

so that the energy is a natural function of the extensive variables S, V, B, and $\mathbf{P}$. The thermodynamic potential is given by the Legendre transformation

$$\Omega(T,V,\mu,\mathbf{v}) = -pV = E - TS - \mu B - \mathbf{v}\cdot\mathbf{P} , \tag{3.16}$$

so that

$$d\Omega = -S\,dT - p\,dV - B\,d\mu - \mathbf{P}\cdot d\mathbf{v} . \tag{3.17}$$

Since the operators appearing in Eq. (3.14) are all diagonal, the thermodynamic potential can be evaluated exactly in this MFT. The results are analogous to those for noninteracting fermions, and with proper care regarding signs, we find

$$\begin{aligned} \Omega(T,V,\mu,\mathbf{v}) &= -T\ln Z \\ &= \tfrac{1}{2}(m_s^2\phi^2 + m_v^2\mathbf{V}^2 - m_v^2 V_0^2)V - T\sum_{k\lambda}[\ln(1+e^{-[E^*(\kappa)-\mathbf{v}\cdot\boldsymbol{\kappa}-\nu]/T}) + \ln(1+e^{-[E^*(\kappa)+\mathbf{v}\cdot\boldsymbol{\kappa}+\nu]/T})] . \end{aligned} \tag{3.18}$$

The sum runs over all single-particle states labeled by momentum $\mathbf{k}$ and intrinsic quantum numbers λ. The *effective chemical potential* ν is defined by

$$\nu \equiv \mu - g_v(V_0 - \mathbf{v}\cdot\mathbf{V}) , \tag{3.19}$$

which is called μ_{eff} in Ref. 30.

The ensemble average of an operator $\hat{A}$ is given by

$$A \equiv \langle\langle\,\hat{A}\,\rangle\rangle = Z^{-1}\mathrm{Tr}(\hat{A}e^{-(\hat{H}-\mu\hat{B}-\mathbf{v}\cdot\hat{\mathbf{P}})/T}) . \tag{3.20}$$

For example, the baryon density is

$$\rho_B \equiv \frac{\langle\langle\,\hat{B}\,\rangle\rangle}{V} = -\frac{1}{V}\left[\frac{\partial\Omega}{\partial\mu}\right] = \frac{1}{V}\sum_{k\lambda}(n_\kappa - \bar{n}_\kappa) . \tag{3.21}$$

Here the partial derivative is taken with all other thermodynamic parameters and field variables held fixed, and we have identified the particle and antiparticle occupation numbers

$$n_\kappa \equiv n_\kappa(T,\nu,\mathbf{v}) = (1+e^{[E^*(\kappa)-\mathbf{v}\cdot\boldsymbol{\kappa}-\nu]/T})^{-1} , \tag{3.22}$$

$$\bar{n}_\kappa \equiv \bar{n}_\kappa(T,\nu,\mathbf{v}) = (1+e^{[E^*(\kappa)+\mathbf{v}\cdot\boldsymbol{\kappa}+\nu]/T})^{-1} . \tag{3.23}$$

By comparing Eq. (3.21) with (3.10), it appears that we can identify the occupation number as the ensemble average of the number operator for each mode. Some care is required, however, with the signs. Notice that

$$\frac{1}{V}\left[\frac{\partial\hat{H}}{\partial M}\right] = \frac{1}{V}\sum_{k\lambda}\frac{M^*}{E^*(\kappa)}(A^\dagger_{k\lambda}A_{k\lambda} + B^\dagger_{-k\lambda}B_{-k\lambda}) \tag{3.24}$$

reproduces the scalar density operator

$$\hat{\rho}_s \equiv V^{-1}\int d^3x\,\bar{\psi}\psi ,$$

except for off-diagonal terms that vanish in the trace. Thus we can compute

$$\begin{aligned} \rho_s &= \frac{1}{V}\langle\langle\,\partial\hat{H}/\partial M\,\rangle\rangle = \frac{1}{V}\left[\frac{\partial\Omega}{\partial M}\right] \\ &= \frac{1}{V}\sum_{k\lambda}\frac{M^*}{E^*(\kappa)}(n_\kappa + \bar{n}_\kappa) . \end{aligned} \tag{3.25}$$

Comparison with Eq. (3.24) now allows us to make the correct identification

$$n_\kappa = \langle\langle\,A^\dagger_{k\lambda}A_{k\lambda}\,\rangle\rangle, \quad \bar{n}_\kappa = \langle\langle\,B^\dagger_{-k\lambda}B_{-k\lambda}\,\rangle\rangle . \tag{3.26}$$

It is now straightforward to express the baryon flux operator in terms of bilinear products of mode operators to find

$$\mathcal{B} = \frac{1}{V}\sum_{k\lambda}\frac{\boldsymbol{\kappa}}{E^*(\kappa)}(n_\kappa + \bar{n}_\kappa) . \tag{3.27}$$

With these results, we can derive equations that determine the meson fields. For a system in equilibrium, these should be chosen to make the thermodynamic potential Ω stationary. For example, $\partial\Omega/\partial\phi = 0$ leads to

$$\phi = \frac{g_s}{m_s^2}\frac{1}{V}\sum_{k\lambda}\frac{M^*}{E^*(\kappa)}(n_\kappa + \bar{n}_\kappa) = \frac{g_s}{m_s^2}\langle\langle\,\hat{\rho}_s\,\rangle\rangle . \tag{3.28}$$

Similarly, the vector field equations become

$$V_0=\frac{g_v}{m_v^2}\frac{1}{V}\sum_{k\lambda}(n_\kappa-\bar{n}_\kappa)=\frac{g_v}{m_v^2}\langle\langle\hat{\rho}_B\rangle\rangle\ , \tag{3.29}$$

$$\mathbf{V}=\frac{g_v}{m_v^2}\frac{1}{V}\sum_{k\lambda}\frac{\boldsymbol{\kappa}}{E^*(\kappa)}(n_\kappa+\bar{n}_\kappa)=\frac{g_v}{m_v^2}\langle\langle\hat{\mathcal{B}}\rangle\rangle\ . \tag{3.30}$$

Thus, by making the thermodynamic potential stationary with respect to the fields, they automatically satisfy the ensemble averages of the normal-ordered field equations resulting from the Lagrangian (3.1).

These relations are extremely useful, for they imply that ϕ and V^μ can be held fixed in computing thermodynamic functions as derivatives of the thermodynamic potential through the relations

$$\begin{aligned}
B&=-\left[\frac{\partial}{\partial\mu}\Omega(T,V,\mu,\mathbf{v})\right]_{T,V,\mathbf{v}}\ ,\\
\mathbf{P}&=-\left[\frac{\partial}{\partial\mathbf{v}}\Omega(T,V,\mu,\mathbf{v})\right]_{T,V,\mu}\ ,\\
S&=-\left[\frac{\partial}{\partial T}\Omega(T,V,\mu,\mathbf{v})\right]_{V,\mu,\mathbf{v}}\ ,\\
p&=-\left[\frac{\partial}{\partial V}\Omega(T,V,\mu,\mathbf{v})\right]_{T,\mu,\mathbf{v}}\ .
\end{aligned} \tag{3.31}$$

Notice that the first two of these relations are satisfied trivially from the definition of the partition function in Eq. (3.14). That is, they will be valid for *any* approximations to the exact Hamiltonian, number operator, and momentum operator. Moreover, since

$$-\left[\frac{\partial\Omega}{\partial T}\right]=\ln Z+\frac{T}{Z}\left[\frac{\partial Z}{\partial T}\right]=\frac{-\Omega+E-\mu B-\mathbf{v}\cdot\mathbf{P}}{T}\ , \tag{3.32}$$

Gibbs' relation (3.16) is satisfied automatically.[35] Finally, since Ω of Eq. (3.18) is linear in V (once the sum has been converted into an integral), Eq. (3.31) merely *defines* the "thermodynamic" pressure. Thus the only real check of the thermodynamic consistency of this approximation is the verification that p defined by Eq. (3.31) agrees with the result computed from the stress tensor in the comoving frame. Since this requires a discussion of the covariance of the preceding results, we postpone this verification until later in this section.

The calculation of the thermodynamic functions in the laboratory frame can now be carried out straightforwardly in this MFT, leading to

$$\rho_s=\frac{\gamma}{(2\pi)^3}\int d^3\kappa\frac{M^*}{E^*(\kappa)}(n_\kappa+\bar{n}_\kappa)\ , \tag{3.33}$$

$$\rho_B=\frac{\gamma}{(2\pi)^3}\int d^3\kappa(n_\kappa-\bar{n}_\kappa)\ , \tag{3.34}$$

$$\mathcal{B}=\frac{\gamma}{(2\pi)^3}\int d^3\kappa\frac{\boldsymbol{\kappa}}{E^*(\kappa)}(n_\kappa+\bar{n}_\kappa)\ , \tag{3.35}$$

$$\mathcal{P}=\frac{g_v^2}{m_v^2}\rho_B\mathcal{B}+\frac{\gamma}{(2\pi)^3}\int d^3\kappa\,\boldsymbol{\kappa}(n_\kappa-\bar{n}_\kappa)\ , \tag{3.36}$$

$$\mathcal{E}=\frac{g_v^2}{2m_v^2}\rho_B^2+\frac{m_s^2}{2g_s^2}(M-M^*)^2+\frac{g_v^2}{2m_v^2}\mathcal{B}^2+\frac{\gamma}{(2\pi)^3}\int d^3\kappa\,E^*(\kappa)(n_\kappa+\bar{n}_\kappa)\ , \tag{3.37}$$

$$p=\frac{g_v^2}{2m_v^2}\rho_B^2-\frac{m_s^2}{2g_s^2}(M-M^*)^2-\frac{g_v^2}{2m_v^2}\mathcal{B}^2-T\frac{\gamma}{(2\pi)^3}\int d^3\kappa[\ln(1-n_\kappa)+\ln(1-\bar{n}_\kappa)]\ , \tag{3.38}$$

$$\sigma=-\frac{\gamma}{(2\pi)^3}\int d^3\kappa[n_\kappa\ln n_\kappa+(1-n_\kappa)\ln(1-n_\kappa)+\bar{n}_\kappa\ln\bar{n}_\kappa+(1-\bar{n}_\kappa)\ln(1-\bar{n}_\kappa)]\ . \tag{3.39}$$

Here γ is the spin-isospin degeneracy, the occupation number distributions are given by Eqs. (3.22) and (3.23), and the meson field equations can be used to write

$$\boldsymbol{\kappa}=\mathbf{k}-\frac{g_v^2}{m_v^2}\mathcal{B}\ , \tag{3.40}$$

$$\nu=\mu-\frac{g_v^2}{m_v^2}(\rho_B-\mathbf{v}\cdot\mathcal{B})\ . \tag{3.41}$$

Note that Eq. (3.28) can be recast as

$$M^*\equiv M-g_s\phi=M-\frac{g_s^2}{m_s^2}\rho_s=M-\frac{g_s^2}{m_s^2}\frac{\gamma}{(2\pi)^3}\int d^3\kappa\frac{M^*}{E^*(\kappa)}(n_\kappa+\bar{n}_\kappa)\ . \tag{3.42}$$

This is a transcendental *self-consistency condition* that determines ϕ.

To compute the thermodynamic functions, one first chooses T, ν, and $\mathbf{v}$. The self-consistency condition (3.42) is then solved to determine M^*. (There may be several solutions for fixed T, ν, and $\mathbf{v}$.) These solutions specify the distribution functions n_κ and $\bar{n}_\kappa$, and the remaining integrals in Eqs. (3.34)–(3.39) can be evaluated directly. At the end of the calculation, one can (in principle) invert these relations to find μ and $\mathbf{v}$ in terms of ρ_B and $\mathcal{P}$, but in practice, desired values of ρ_B and $\mathcal{P}$ are found by searching on values of ν and $\mathbf{v}$. Similarly, to compute results at fixed entropy, it is easiest to search through values of T.

In the $\mathbf{v}\to 0$ limit, the distribution functions reduce to

$$\begin{Bmatrix} n_\kappa(T',\nu',0)\\ \bar{n}_\kappa(T',\nu',0)\end{Bmatrix}=(1+e^{[E^*(k)\mp\nu']/T'})^{-1}\equiv\begin{Bmatrix} n'_k(T',\nu')\\ \bar{n}'_k(T',\nu')\end{Bmatrix}\ . \tag{3.43}$$

Here we follow our "prime" notation, since the observer

is now in the comoving frame. There is no angular dependence in the distribution functions, so $\mathcal{B}=\mathcal{P}=0$, and this allows us to replace κ with k. The distribution functions (3.43) agree with those in Eqs. (3.77) and (3.78) of Ref. 10, and our Eqs. (3.33), (3.34), and (3.37) become

$$\rho_s'=\frac{\gamma}{(2\pi)^3}\int d^3k\frac{M^*}{E^*(k)}(n_k'+\bar{n}_k') , \tag{3.44}$$

$$\rho_B'=\frac{\gamma}{(2\pi)^3}\int d^3k(n_k'-\bar{n}_k') , \tag{3.45}$$

$$\mathcal{E}'=\frac{g_v^2}{2m_v^2}(\rho_B')^2+\frac{m_s^2}{2g_s^2}(M-M^*)^2 + \frac{\gamma}{(2\pi)^3}\int d^3k\, E^*(k)(n_k'+\bar{n}_k') . \tag{3.46}$$

For the pressure, the integrand in Eq. (3.38) is now spherically symmetric, which allows us to perform a partial integration, yielding

$$p=\frac{g_v^2}{2m_v^2}(\rho_B')^2-\frac{m_s^2}{2g_s^2}(M-M^*)^2 + \frac{1}{3}\frac{\gamma}{2\pi^2}\int_0^\infty dk\frac{k^4}{E^*(k)}(n_k'+\bar{n}_k') . \tag{3.47}$$

These expressions agree with Eqs. (3.74)–(3.76) of Ref. 10, and Eq. (2.24) is satisfied at $T=0$. It is also a simple matter to show that (3.47) agrees with the trace of the stress tensor evaluated in the comoving frame: $p=\frac{1}{3}\langle\langle \hat{T}'_{i'i'}\rangle\rangle$. To derive this last result, use Eqs. (3.3), (3.8), and (3.9), and remember to normal order the operators for negative-energy states. Thus, at least for $\mathbf{v}=0$, the MFT is thermodynamically consistent.

Let us now return to finite relative velocity and take the $T\to 0$ limit. Since $E^*(\kappa)\geq\kappa$ and $|\mathbf{v}\cdot\boldsymbol{\kappa}|<\kappa$, it follows that $E^*(\kappa)\pm\mathbf{v}\cdot\boldsymbol{\kappa}>0$. If we consider only systems with $\nu\geq 0$ (no net antibaryons), the antibaryon distribution goes to zero in this limit, while the baryon distribution becomes unity for $E^*(\kappa)-\mathbf{v}\cdot\boldsymbol{\kappa}-\nu<0$ and zero otherwise.[36] Thus the (nonspherical) Fermi surface is defined by

$$E^*(\kappa_F)-\mathbf{v}\cdot\boldsymbol{\kappa}_F=\nu , \tag{3.48}$$

in agreement with Eq. (2.9) of Ref. 30 and the minimization condition discussed at the beginning of this section [Eq. (3.13)]. The preceding results for ρ_s, ρ_B, $\mathcal{B}$, and $\mathcal{P}$ then reduce immediately to those in Eqs. (2.12)–(2.15) of Ref. 30, and it is easy to verify that the entropy density σ is identically zero. For the pressure, some care must be used in the limit, since

$$\lim_{T\to 0} T\ln(1-n_\kappa)=E^*(\kappa)-\mathbf{v}\cdot\boldsymbol{\kappa}-\nu =E^*(\kappa)-\mathbf{v}\cdot\mathbf{k}-\mu+\frac{g_v^2}{m_v^2}\rho_B \tag{3.49}$$

for occupied states in the Fermi sea. When used in conjunction with the preceding zero-temperature results [see also Eqs. (2.29)–(2.32) in Ref. 30], it follows that

$$p=\eta^2\mu\rho_B-\mathcal{E} . \tag{3.50}$$

As we will see, this is the correct representation of the (Lorentz scalar) p in terms of laboratory-frame quantities.

We now prove the Lorentz covariance of the expressions in Eqs. (3.33)–(3.39) by making a suitable change of integration variables. Not surprisingly, this change of variables looks like a Lorentz transformation to the comoving frame. Let us define two new momenta $\mathbf{t}$ and $\mathbf{q}$ related to $\boldsymbol{\kappa}$ by

$$\boldsymbol{\kappa}\equiv\mathbf{t}+\frac{\eta^2\mathbf{v}}{1+\eta}\mathbf{v}\cdot\mathbf{t}+\eta\mathbf{v}E^*(t) , \qquad \boldsymbol{\kappa}\equiv\mathbf{q}+\frac{\eta^2\mathbf{v}}{1+\eta}\mathbf{v}\cdot\mathbf{q}-\eta\mathbf{v}E^*(q) . \tag{3.51}$$

The variable $\mathbf{t}$ will be used to rewrite the integrals over the particle distributions, while $\mathbf{q}$ will be used for the antiparticle distributions. [Recall that $\eta=(1-v^2)^{-1/2}$.] The parameter M^* appearing in E^* can be given its value in the laboratory frame, but we will find that this is a scalar, as expected. It is a straightforward matter of algebra to show that

$$E^*(\kappa)=\eta[E^*(t)+\mathbf{v}\cdot\mathbf{t}], \quad E^*(\kappa)=\eta[E^*(q)-\mathbf{v}\cdot\mathbf{q}] , \tag{3.52}$$

and to compute the Jacobians

$$d^3\kappa=\eta\left[1+\frac{\mathbf{v}\cdot\mathbf{t}}{E^*(t)}\right]d^3t, \quad d^3\kappa=\eta\left[1-\frac{\mathbf{v}\cdot\mathbf{q}}{E^*(q)}\right]d^3q . \tag{3.53}$$

Consider now the Fermi distribution function for particles under the change of variables $\boldsymbol{\kappa}\to\mathbf{t}$. Since Eqs. (3.51) and (3.52) imply that

$$E^*(\kappa)-\mathbf{v}\cdot\boldsymbol{\kappa}=E^*(t)/\eta ,$$

we can rewrite the distribution as

$$n_\kappa(T,\nu,\mathbf{v})=(1+e^{[E^*(t)-\eta\nu]/\eta T})^{-1}=n_t'(\eta T,\eta\nu) , \tag{3.54}$$

with n_t' given by Eq. (3.43). With this change of variables, the particle distribution function looks just like a comoving-frame distribution function (i.e., no angular dependence) with the thermodynamic variables [compare Eq. (3.43)]

$$T'\equiv\eta T, \quad \nu'\equiv\eta\nu . \tag{3.55}$$

In other words, if we *define* the transformation properties of the temperature and chemical potential as in Eq. (3.55), the distribution function $n_\kappa(T,\nu,\mathbf{v})$ is a Lorentz scalar. This is as it should be, since all observers must agree on the occupation probability of a given single-

particle state. Similarly, the antiparticle distribution function becomes

$$\bar{n}_\kappa(T,\nu,\mathbf{v})=(1+e^{[E^*(q)+\eta\nu]/\eta T})^{-1}=\bar{n}'_q(\eta T,\eta\nu)\ . \quad (3.56)$$

The proof of Lorentz covariance now proceeds easily. To illustrate the procedure with a nontrivial example, consider the baryon flux $\mathcal{B}$. To simplify the expressions, we take $\mathbf{v}\|\hat{z}$, so that

$$\begin{aligned}\mathcal{B}_z&=\frac{\gamma}{(2\pi)^3}\int d^3\kappa\frac{\kappa_z}{E^*(\kappa)}(n_\kappa+\bar{n}_\kappa)\\&=\frac{\gamma}{(2\pi)^3}\left\{\int d^3t\, n'_t\eta\left[1+\frac{vt_z}{E^*(t)}\right]\eta[t_z+vE^*(t)]\left[\eta E^*(t)\left[1+\frac{vt_z}{E^*(t)}\right]\right]^{-1}\right.\\&\quad\left.+\int d^3q\,\bar{n}'_q\eta\left[1-\frac{vq_z}{E^*(q)}\right]\eta[q_z-vE^*(q)]\left[\eta E^*(q)\left[1-\frac{vq_z}{E^*(q)}\right]\right]^{-1}\right\}\\&=\frac{\gamma}{(2\pi)^3}(\eta v\int d^3t\, n'_t-\eta v\int d^3q\,\bar{n}'_q)=\eta v\rho'_{\mathrm{B}}\ .\end{aligned} \quad (3.57)$$

Since the transformed distribution functions n'_t and $\bar{n}'_q$ are spherically symmetric, all integrals linear in $\mathbf{t}$ or $\mathbf{q}$ vanish, and we have identified the proper baryon density ρ'_{B} [Eq. (3.45)] in the final expression. With similar techniques and Eqs. (3.44)–(3.47), it is easy to show that

$$\begin{aligned}&\rho_{\mathrm{s}}=\rho'_{\mathrm{s}},\quad \rho_{\mathrm{B}}=\eta\rho'_{\mathrm{B}},\quad \sigma=\eta\sigma'\ ,\\&\mathcal{E}=\eta^2(\mathcal{E}'+v^2p),\quad \mathcal{P}=\eta^2\mathbf{v}(\mathcal{E}'+p)\ .\end{aligned} \quad (3.58)$$

Equations (3.57) and (3.58) verify that ρ_{s} is a scalar, ρ_{B} and $\mathcal{B}$ are the components of a four-vector B^μ, σ is the timelike component of a four-vector S^μ, and $\mathcal{E}=T^{00}$ and $\mathcal{P}^i=T^{0i}$ are components of the energy-momentum tensor $T^{\mu\nu}$, all defined correctly in terms of comoving-frame ("secondary") quantities by Eqs. (2.10) and (2.17)–(2.19). (The transformation of the spacelike components T^{ij} can be verified analogously.)

All that is left to show is that the pressure in Eq. (3.38) is indeed a Lorentz scalar. In other words, the evaluation of (3.38) with parameters T, ν, and $\mathbf{v}$ should lead to precisely the same result as the comoving-frame formula evaluated with $T'=\eta T$ and $\nu'=\eta\nu$. This conclusion follows by inspection of Eq. (3.38). With the change of variables in Eq. (3.51), the distribution functions are spherically symmetric, so terms in the Jacobians (3.53) that are linear in the momenta again vanish. This leaves an integral that contains the new distribution functions (3.54) and (3.56), multiplied by a factor of η, which combines with the existing factor of T to yield the desired T'. Thus the final term in Eq. (3.38) is a scalar. Since M^* is a scalar, as is $\rho_{\mathrm{B}}^2-\mathcal{B}^2=B^\mu B_\mu$, the remaining terms are also scalars, verifying the desired result.

The proof of Lorentz covariance is now complete. The primary thermodynamic functions computed for the moving fluid are correctly described in terms of the transformed secondary thermodynamic functions of Sec. II. This also verifies the thermodynamic consistency of the MFT in all frames, since we know from Eq. (3.47) that the pressure evaluated from the stress tensor in the comoving frame agrees with Gibbs' relation (2.22). Moreover, this implies that at zero temperature, $p=\mu'\rho'_{\mathrm{B}}-\mathcal{E}'$; when combined with the transformations (3.55) and (3.58), the laboratory-frame expression [Eq. (3.50)] for p is obtained. Most importantly, as shown in Sec. II, since the MFT is both thermodynamically consistent and Lorentz covariant, the covariant thermodynamic relations (2.20), (2.26), and (2.27) are all guaranteed to hold. In particular, Eqs. (3.15) and (3.16) at constant volume follow from the zeroth components of Eqs. (2.20) and (2.26), together with the transformation laws in Eq. (3.55). The verification of these relations from the explicit expressions (3.34)–(3.39) is left as an exercise for the reader. It is also left as an exercise to show that these expressions can be rewritten in a manifestly covariant form.[25]

We turn now to the partition function defined in Eq. (3.14), and show that this is consistent with the covariant definition in Eq. (2.30). Since the system is uniform, the partition function can be written in terms of density operators as

$$Z=\mathrm{Tr}\exp\left[-\frac{1}{T}\int d^3x(\hat{\mathcal{H}}-\mu\hat{\rho}_{\mathrm{B}}-\mathbf{v}\cdot\hat{\mathcal{P}})\right]\ . \quad (3.59)$$

We emphasize that all quantities in this expression are defined in the laboratory frame. In particular, the operators are constructed from baryon fields that satisfy (3.9) at equal times observed in this frame. By writing the inverse temperature as $1/T=\eta/T'\equiv\eta\beta$ and defining the thermal potential as $\alpha\equiv\mu/T=\mu'/T'$, Eq. (3.59) becomes

$$\begin{aligned}Z&=\mathrm{Tr}\exp\left[-\int d^3x[\beta\eta(\hat{T}^{00}-v^i\hat{T}^{i0})-\alpha\hat{\rho}_{\mathrm{B}}]\right]\\&=\mathrm{Tr}\exp\left[-\int d^3x\,\delta_{\mu0}(\beta_\nu\hat{T}^{\nu\mu}-\alpha\hat{B}^\mu)\right]\ .\end{aligned} \quad (3.60)$$

Here we have identified the Hamiltonian density and momentum density operators as components of the laboratory-frame energy-momentum tensor and have defined a thermal four-vector β^μ as in Eq. (2.11). If we now define the purely spacelike hypersurface element in the laboratory frame as $d\Lambda_\mu\equiv d^3x\,\delta_{\mu0}$, Eq. (3.60) reproduces Eq. (2.30).

There are several important points to note. First, the preceding derivation shows that the canonical evaluation

of the partition function yields a Lorentz scalar, which is the reason for the covariance of the MFT results. Moreover, the partition function defined by Eq. (2.30) is a scalar for *any* spacelike hypersurface Λ_μ. Indeed, since quantization can be performed on any Λ_μ with equivalent results,[32,33] one can even choose *different hypersurfaces in different reference frames,* as long as the operators $\hat{B}^\mu$ and $\hat{T}^{\mu\nu}$ are quantized on the appropriate hypersurface in each frame.

This is precisely how we performed the MFT calculation. Equation (3.9) implies that the quantization was carried out on the purely spacelike Λ_μ in the laboratory frame; if Eq. (2.30) was rewritten in the comoving frame using the same Λ_μ, the resulting expression would look quite unfamiliar. As we proved, however, covariance is maintained even when the comoving-frame results are computed by quantizing on the purely spacelike hypersurface *in that frame,* as in Ref. 10. Thus we have not only justified the definition (2.30), which allows the partition function to be computed directly in any reference frame, but have also learned that Λ_μ can be chosen to make the computation as simple as possible. This last result is usually overlooked in the literature.[2,14]

IV. DISCUSSION

Thus far we have described how to calculate nuclear matter properties in an arbitrary frame and examined some consequences of thermodynamic consistency. We now want to illustrate these results by considering some simple models of finite-temperature nuclear systems. We will concentrate on bulk nuclear properties and use a hydrodynamic approach, since this gives the most direct connection to the thermodynamic variables.

Because of the simplicity of our model Lagrangian (3.1), the mean-field approximation of Sec. III, and a hydrodynamic description of the evolution, the results that follow will only be qualitatively accurate. These three major simplifications can be relaxed, however, and more detailed calculations can be performed using techniques similar to those discussed earlier. We use the simpler, more familiar approaches to illustrate which thermodynamic variables are relevant, and to concentrate on new aspects that arise from a covariant description of the matter. In particular, the covariant formulation elevates the fluid velocity $\mathbf{v}$ and its conjugate, the momentum density $\mathcal{P}$, to the status of thermodynamic parameters, and we study the role of these parameters in the description of moving systems. We expect that the general features of our discussion will remain valid in more sophisticated calculations.

A. Heavy-ion collisions

In a hydrodynamic description of a heavy-ion collision, the basic equations for energy flow, momentum flow, and matter flow follow from the conservation laws (2.4) for the baryon current and the energy-momentum tensor.[37] These equations can be written in the laboratory frame as

$$\frac{\partial \mathcal{E}}{\partial t}+\nabla\cdot(\mathbf{v}\mathcal{E})=-\nabla\cdot(\mathbf{v}p)\ , \tag{4.1}$$

$$\frac{\partial \mathcal{P}}{\partial t}+(\mathbf{v}\cdot\nabla)\mathcal{P}+\mathcal{P}(\nabla\cdot\mathbf{v})=-\nabla p\ , \tag{4.2}$$

$$\frac{\partial \rho_B}{\partial t}+\nabla\cdot(\mathbf{v}\rho_B)=0\ , \tag{4.3}$$

where we first introduced the secondary quantities defined in Eqs. (2.17) and (2.19) and then used the Lorentz transformation properties in (3.57) and (3.58). We assume that the fluid is "perfect," so that it appears isotropic to an observer in the comoving frame, and all contributions from viscosity, dissipation, etc., have been neglected. A basic assumption of the hydrodynamic model is that local thermodynamic properties of the matter (for example, ρ_B, $\mathcal{E}$, and p) can be computed from the infinite system, as in Sec. III.

In the usual approach, one specifies some initial conditions and solves Eqs. (4.1)–(4.3) for the physically relevant *proper* quantities p, ρ_B', and $\mathcal{E}'$, together with the local fluid velocity $\mathbf{v}$. Since there are six unknowns and five equations, an additional relation is required to obtain a solution. This is provided by the equation of state, which can be written as

$$\mathcal{E}'=\mathcal{E}'(\rho_B',T'),\quad p=p(\rho_B',T') \tag{4.4}$$

in the comoving frame. The proper temperature T' has been introduced as a parametric variable, so there are now seven equations in seven unknowns. Note that the entropy/baryon (S/B) could have been used instead of T'.

One reason for expressing the hydrodynamic solutions in terms of proper variables is that, typically, the equation of state (4.4) can be calculated only in the rest frame of the matter. In a covariant approach, however, one can dispense with the boost relations and solve the hydrodynamic equations directly in the laboratory frame, using $\mathcal{E}$ and p computed as functions of ρ_B, T or σ, and $\mathbf{v}$ or $\mathcal{P}$. Thus $\mathcal{P}$ can be replaced by $\mathcal{P}=\mathbf{v}(\mathcal{E}+p)$, which follows from Lorentz covariance [see Eq. (3.58)], and p can be eliminated in favor of $\mathcal{E}$.

The equation of state (EOS) for nuclear matter ($\gamma=4$) in the mean-field model of Sec. III is shown in Figs. 1 and 2. Note that the EOS is defined in terms of the *proper* energy density, as in (4.4), and we show results for both isotherms and isentropes. The MFT thermodynamic quantities depend only on the ratios of couplings to masses, and we choose[38]

$$C_s^2\equiv g_s^2(M^2/m_s^2)=357.4,\quad C_v^2\equiv g_v^2(M^2/m_v^2)=273.8\ , \tag{4.5}$$

which produce zero-temperature equilibrium at $k_F=1.30$ fm^{-1}, with a binding energy of 15.75 MeV and a compressibility of $K=545$ MeV. At low density, there is a liquid-gas (van der Waals) phase transition, and at high density, the system approaches the causal limit $p=\mathcal{E}'$. If $\rho_B'\to\infty$ at any T', the system becomes degenerate, and the zero-temperature results are obtained. If $T'\ll M$ and $\rho_B'\to 0$, the system resembles a classical nonrelativistic gas [$p=\frac{2}{3}(\mathcal{E}'-M\rho_B')$], while if $T'\to\infty$ at any ρ_B', baryon-antibaryon pairs will be produced, and the EOS is that of a black body ($p=\frac{1}{3}\mathcal{E}'$).

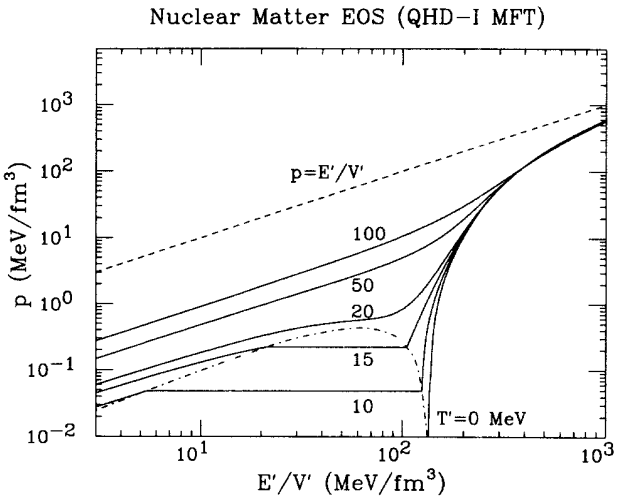

FIG. 1. Nuclear matter equation of state on isotherms. The dashed line represents the causal limit, and the dotted-dash line is the liquid-gas coexistence curve. The solid curves are labeled by the proper temperature.

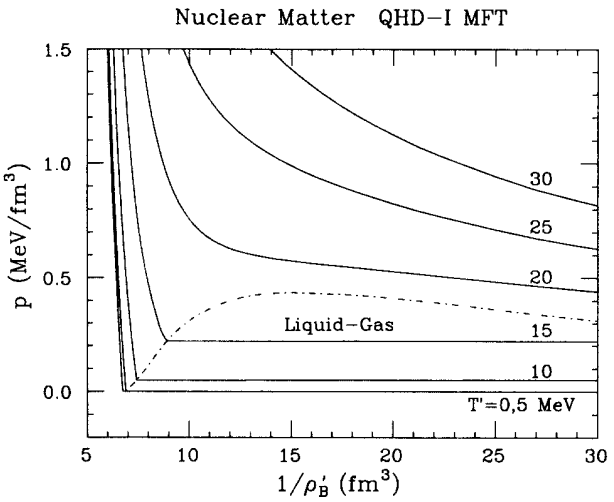

FIG. 3. Nuclear matter phase diagram: pressure as a function of proper volume/baryon for various proper temperatures. The dotted-dash line is the liquid-gas coexistence curve.

Figure 3 shows the nuclear matter phase diagram, and the dotted-dash line gives the phase coexistence boundary. This is determined by Gibbs' criteria, namely, that the liquid and gas phases have equal temperatures (thermal equilibrium), chemical potentials (chemical equilibrium), and pressures (hydrostatic equilibrium). Below the coexistence curve, the equilibrium state is a mixture of gas and liquid. The critical temperature in this model is roughly 18.3 MeV, which is similar to that obtained in other models that reproduce the empirical saturation point.[39–43] This similarity occurs even though the present model has a rather large compressibility. (If the nonlinear mean-field model of Ref. 44 is used, which has a compressibility of $K \approx 225$ MeV, the critical temperature is ≈ 14.2 MeV.)

The density and temperature dependence of the baryon effective mass M^* is illustrated in Fig. 4. For low temperatures, the density dependence is more important than the temperature dependence. As the temperature is increased, M^* first increases and then decreases rapidly for $T' \approx 200$ MeV. (This is true except at very small densities, where M^* decreases monotonically with tempera-

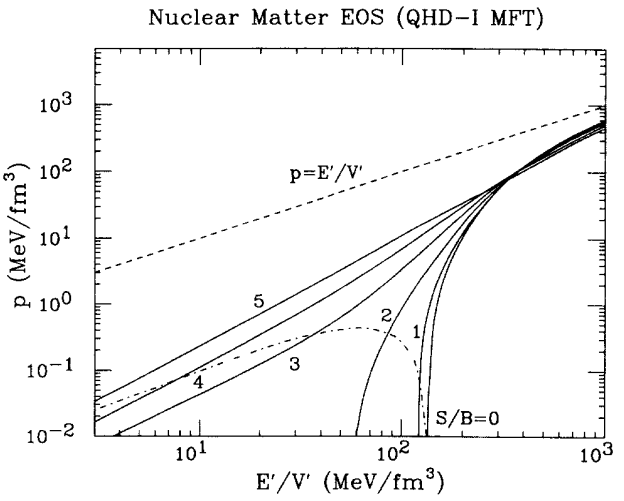

FIG. 2. Nuclear matter equation of state on isentropes. The dashed line represents the causal limit, and the dotted-dash line is the liquid-gas coexistence curve. The solid curves are labeled by the entropy/baryon.

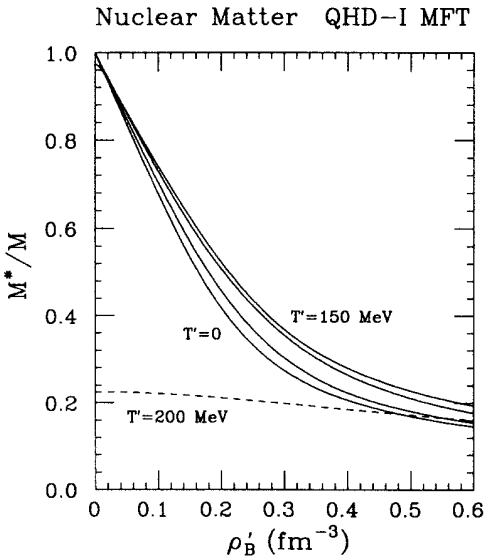

FIG. 4. Baryon effective mass in nuclear matter as a function of the proper baryon density and temperature. The solid curves show results for $T' = 0$, 50, 100, and 150 MeV.

ture.) This rapid decrease of M^* with increasing temperature resembles a phase transition, and at high temperature and low density, the system becomes a dilute gas of baryons in a sea of baryon-antibaryon pairs. This behavior is also indicated in Fig. 5, which shows the entropy density as a function of baryon density for various temperatures.

We remark that at high temperatures ($T' \gtrsim 100$ MeV), the equation of state in Figs. 1 and 2 will be modified by contributions from thermal pions, which are not included here. Moreover, at very high temperature or density, the hadrons will dissolve into a quark-gluon plasma, through what is now believed to be a first-order phase transition.[45,46] One goal of QHD is to describe the hadronic phase of this system accurately and identify signals of the QCD phase transition. However, if the hadronic phase becomes an essentially massless gas with high entropy density *before* the transition to quarks and gluons, the unambiguous observation of the latter transition will be difficult. In particular, it is impossible to associate the small baryon mass (sometimes characterized as "chiral symmetry restoration") with the onset of the quark-gluon phase, if the mass already becomes small in the hadronic phase.

Let us now consider lower temperatures and focus on medium-energy heavy-ion collisions, which can give us information on the liquid-gas phase transition. Starting with two nuclei colliding in their c.m. frame, one can follow the evolution by solving the hydrodynamic equations (or some more sophisticated equations) using the nuclear EOS (or the NN interaction) as input. We will assume that the combined system is compressed and heated (due to the formation of a shock front) and ultimately reaches thermal equilibrium at some finite temperature, density, and pressure. Whether the system actually reaches equilibrium in these collisions is a difficult question that is clearly beyond the scope of our simple model; for illustration, we will simply assume that such a state occurs.

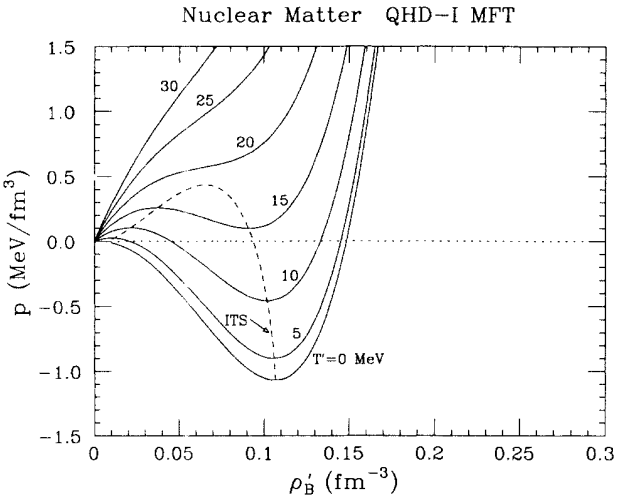

FIG. 6. Pressure as a function of proper baryon density for various temperatures. The isothermal spinodal (ITS), which is defined by $(\partial p/\partial \rho_B')_{T'}=0$, is indicated by the dashed curve.

The properties of the resulting equilibrium system can be deduced from Figs. 6 and 7, where the pressure and energy/baryon are shown as functions of the proper density for various temperatures. If the reaction is observed from the c.m. frame, the equilibrium system is created at rest. However, since $p>0$, the system is not in hydrostatic equilibrium and will expand; moreover, since the hot nucleus is not in thermal equilibrium with its surroundings, it will cool down. We are basically interested in the evolution of this expanding, hot nuclear matter.

The evolution can be related to the thermodynamic variables by studying Fig. 8, which illustrates properties of the system in the temperature-density plane. Equipotential surfaces of constant energy/baryon and lines of

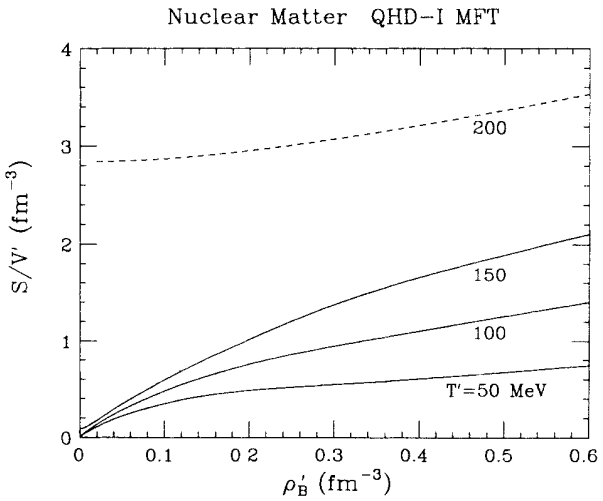

FIG. 5. Proper entropy density as a function of proper baryon density for various temperatures.

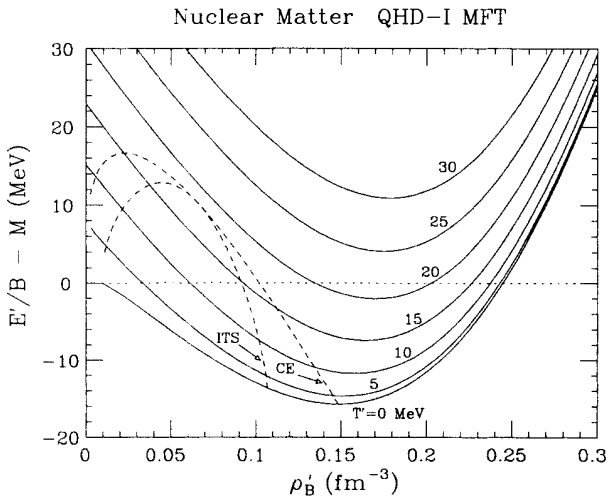

FIG. 7. Proper energy/baryon as a function of baryon density for various temperatures. The isothermal spinodal (ITS) and liquid-gas coexistence curve (CE) are indicated.

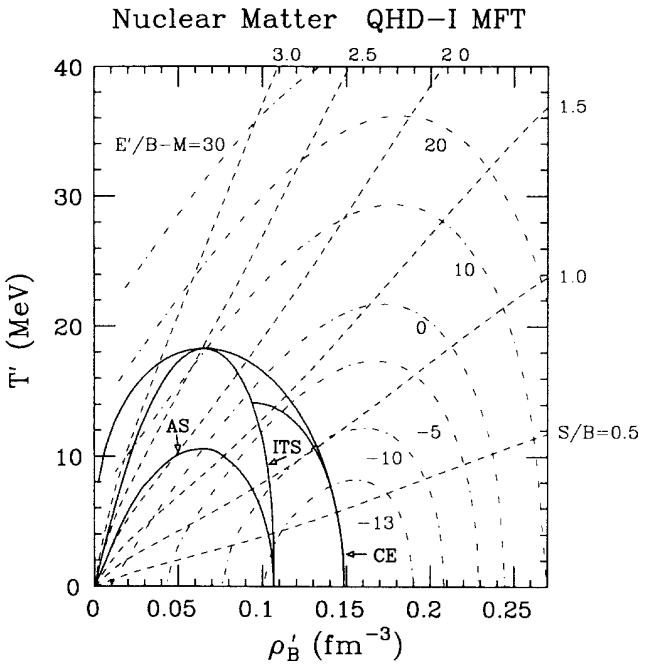

FIG. 8. Properties of nuclear matter as functions of temperature and density in the comoving frame. The dotted-dashed curves are contours of equal energy/baryon (in MeV), and adiabats are shown as dashed curves. The solid curves determine the phase separation and are described in the text.

constant entropy/baryon (adiabats) are shown. The properties of the system along the adiabats can be deduced from Figs. 9 and 10, which indicate the pressure and energy/baryon as functions of the density for various values of the entropy/baryon.

The four solid curves in the lower left corner of Fig. 8

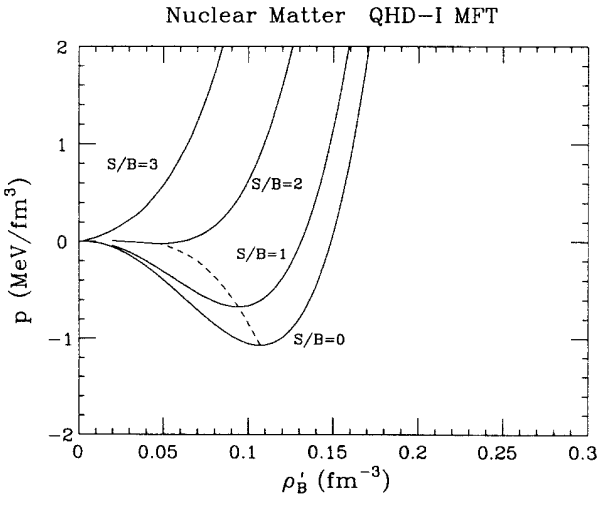

FIG. 9. Pressure as a function of proper baryon density for several values of the entropy/baryon. The adiabatic spinodal, defined by $(\partial p/\partial \rho_B')_{S/B}=0$, is indicated by the dashed line.

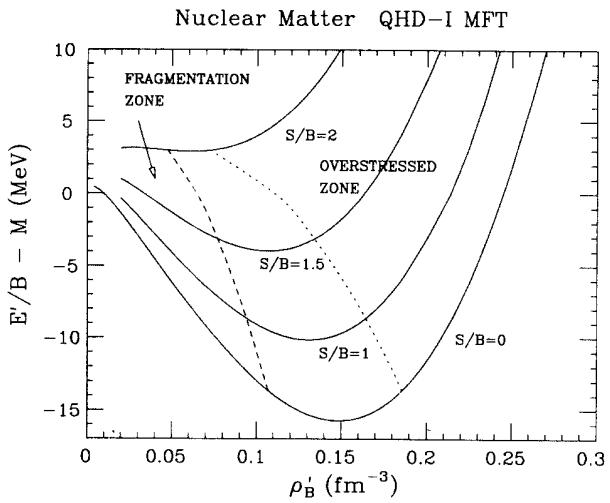

FIG. 10. Proper energy/baryon as a function of density for several values of the entropy/baryon. The dashed line is the adiabatic spinodal, and the fragmentation zone represents the region of mechanical instability. If the hot equilibrium nucleus is formed in the "overstressed zone" to the right of the dotted curve, subsequent isentropic expansion will lead to fragmentation.

describe the phase transition. The outer curve is the coexistence (CE) curve, which is determined by Gibbs' phase criteria discussed earlier. Inside the CE curve, the thermodynamically stable system is a mixture of liquid and gas. We also show the isothermal spinodal (ITS), which intersects the coexistence curve at the critical temperature. The ITS is defined by the locus $(\partial p/\partial \rho_B')_{T'}=0$ and can be deduced from Fig. 6, where this locus is shown. Similarly, the innermost solid curve is the adiabatic spinodal (AS), which is defined by $(\partial p/\partial \rho_B')_{S/B}=0$, and which follows from the dashed curve in Fig. 9.

Between the CE curve and the spinodals, $\partial p/\partial \rho_B' > 0$; thus the system is stable against small density fluctuations, and it may become superheated. When the system crosses a spinodal, however, $\partial p/\partial \rho_B'$ becomes negative, and instability to small fluctuations is possible, leading immediately to fragmentation. This is believed to occur by the formation of droplets surrounded by vapor.[39,47] The remaining (unlabeled) solid curve in Fig. 8 shows the points of hydrostatic equilibrium ($p=0$) at constant temperature; the intersection of this curve with the ITS is known as the "flash point" and represents the highest temperature at which a self-bound system can exist in hydrostatic equilibrium. (In this model, $T_{\rm flash} \approx 14.1$ MeV.) In contrast, equilibrium points at constant entropy/baryon occur when an adiabat is tangent to an equipotential surface.

The expansion of the hot nucleus is a complex process that involves the interplay of the hydrodynamic relations in Eqs. (4.1)–(4.3), augmented to include various transport coefficients and nonequilibrium effects, such as nucleation and fragmentation. To simplify the discussion, we can consider two limiting cases: isoergic expansion and isentropic expansion.[48] As the system expands, internal energy is transformed into collective motion, which

manifests itself as local flow velocity. If the expansion is highly damped, the energy of motion is rapidly transformed back into internal energy; the resulting expansion is therefore slow and proceeds along an equipotential surface. The expansion proceeds until $p=0$, after which the fluid remains at rest and evaporates particles until it is cool. In contrast, if the motion is undamped, the expansion carries the system past hydrostatic equilibrium, where it begins to slow down as the energy of motion is returned to internal energy. Since there is no dissipation, the expansion is isentropic, and the motion is bounded by the equipotential surface of the initial hot configuration. Intranuclear cascade calculations suggest that the expansion is nearly isentropic.[40,49]

Consider the isentropic expansion of a system with relatively low excitation and entropy/baryon, say, $S/B \approx 1.0$. As the system expands into the coexistence region, several outcomes are possible. The evolution depends on the relative rates of expansion and nucleation.[39,48] If the expansion is slow enough to allow for nucleation, bubbles of gas form or the system fragments into droplets and vapor. If the nucleation is relatively slow, which is more likely, the system will become superheated. If the expansion halts before the adiabatic spinodal is reached, the direction of motion is reversed and the system vibrates, ultimately evaporating nucleons to cool down. In contrast, if the system crosses the adiabatic spinodal, fragmentation occurs. Initial conditions that produce this fragmentation in the present model are denoted by the "overstressed zone" in Fig. 10.

If the initial entropy is high enough, the system crosses the CE curve but misses the AS and simply vaporizes. Of course, since it is already unbound (in this model), it is evaporating particles all the while.

During the expansion, both the local velocity and momentum/baryon will be nonzero. Our covariant analysis shows that these are conjugate variables, just like T and S. Which of these is the relevant thermodynamic variable for the expansion?

To answer this question, it is useful to introduce the "hydrodynamic mass" $M_{\rm hyd}$, which relates v to P/B.[10,30] An expression for $M_{\rm hyd}$ can be deduced solely from thermodynamics and Lorentz covariance. By combining the expressions for $\mathcal{E}$ and $\mathcal{P}$ in the boost relations (3.58), one discovers $\mathcal{P}=\mathbf{v}(\mathcal{E}+p)$. This equality can be divided by $\rho_{\rm B}$ to give a relation for $M_{\rm hyd}$, and Eq. (2.22), which is a consequence of the first law of thermodynamics, produces another useful result:

$$M_{\rm hyd} \equiv \frac{P/B}{v} = \frac{\mathcal{E}+p}{\rho_{\rm B}} = \eta \left[T' \left(\frac{S}{B} \right) + \mu' \right] . \tag{4.6}$$

To see why this should be interpreted as a "hydrodynamic mass," insert $\mathcal{P}=\rho_{\rm B}\mathbf{v}M_{\rm hyd}$ into the momentum flow equation (4.2). Note that $\rho_{\rm B}$ is the number density of baryons. If we use the energy flow equation (4.1) and the continuity equation (4.3), we find

$$\frac{\partial \mathbf{v}}{\partial t} + (\mathbf{v}\cdot\nabla)\mathbf{v} = -\frac{1}{\rho_{\rm B} M_{\rm hyd}} \left[\nabla p + \mathbf{v} \frac{\partial p}{\partial t} \right] . \tag{4.7}$$

This will be recognized as Euler's equation for hydrodynamic flow,[27,50] which embodies the content of Newton's second law, if we identify the "mass density" of the fluid as $\rho_{\rm B} M_{\rm hyd}$. Thus, $M_{\rm hyd}$ is the relevant parameter for describing the inertia of the flowing system.

There are several important features of the hydrodynamic mass.

(i) It arises naturally in the present covariant approach when one calculates thermodynamic properties in an arbitrary reference frame.

(ii) As is clear from the final expression in Eq. (4.6), $M_{\rm hyd}$ is not really a mass at all, since it transforms like an energy. (Recall that T', μ', S, and B are all Lorentz scalars.) It is more appropriate to call it the "hydrodynamic potential," but in an abuse of terminology, we will use "mass" and "potential" interchangeably in the sequel.

(iii) $M_{\rm hyd}$ gives the ratio between P/B and v and is the inertia parameter for the moving system. It is a dynamical quantity that depends on the equation of state. It is *incorrect* to relate P/B and v using the nucleon mass M or the effective mass M^*. In the comoving frame at zero temperature, $M_{\rm hyd}=\mu' \approx M$, which explains why isoscalar nuclear magnetic moments reproduce the Schmidt lines in the relativistic MFT.[30,44]

(iv) The hydrodynamic mass in the present model is shown in Fig. 11 as a function of the (proper) density and temperature. $M_{\rm hyd}$ becomes large in a variety of situations: If $\rho_{\rm B} \to \infty$ at any temperature, the system becomes a dense, degenerate Fermi gas dominated by vector repulsion, which stiffens the EOS. If $T \to \infty$ at any density, the system becomes a nucleon-antinucleon plasma with a large inertia. If $S/B \to \infty$ at any (finite) temperature, the resulting classical gas has a large inertia. If $v \to \infty$ at any T' and μ', the rapidly moving system also has a large inertia.

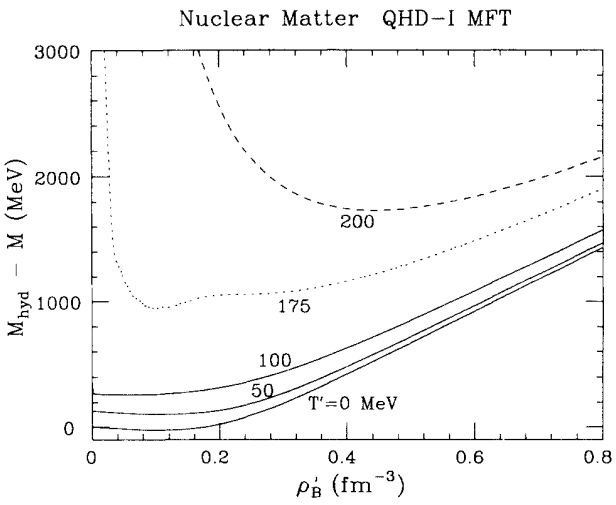

FIG. 11. The "hydrodynamic mass" $M_{\rm hyd}$ as a function of the proper density for several temperatures. These values of $M_{\rm hyd}-M$ are computed with $v=0$; the results in an arbitrary frame are given by adding M and multiplying by η.

(v) Using Eq. (4.6), we can define the hydrodynamic potential explicitly as

$$BM_{\rm hyd} \equiv BM_{\rm hyd}(S,\ p,\ B,\ \mathbf{P}) = E + pV\ . \tag{4.8}$$

Notice that S, p, and B are Lorentz scalars, and thus the value of $M_{\rm hyd}$ in different frames is determined solely by its dependence on $\mathbf{P}$.

Having defined the hydrodynamic potential, we still must decide whether $\mathbf{v}$ or $\mathcal{P}$ is the relevant variable to describe the expansion of the hot nucleus. Since the collective motion of the system is described by Euler's equation (4.7), the pressure gradients drive the motion. Thus, neither v nor P will be constant as the hot system expands, regardless of whether it oscillates or reaches the AS and fragments. In Fig. 12, we show the adiabatic spinodal as a function of density and momentum/baryon for fixed $S/B = 1$. [In other words, the solid curve is the locus $(\partial p/\partial \rho_{\rm B})_{S/B=1,P/B} = 0$. The intersection of the $S/B = 1$ adiabat with the AS in Fig. 8 gives the result at $P/B = 0$.] The dotted curves in the figure show the fluid velocities associated with given $\rho_{\rm B}$ and P/B. Since $M_{\rm hyd}$ is essentially constant for these temperatures and densities (see Figs. 8 and 11), the velocity curves are also essentially constant, and it is immaterial whether we use v or P/B to describe the expansion. [In fact, the adiabatic spinodal at constant velocity, $(\partial p/\partial \rho_{\rm B})_{S/B=1,v} = 0$, is also plotted in Fig. 12, but it is indistinguishable from the solid curve.] Moreover, since $M_{\rm hyd} \approx \mu \approx M$ in this temperature and density regime, taking $\mathbf{P} = MB\mathbf{v}$, as is usually done in nonrelativistic calculations, introduces negligible errors. These results would follow automatically if one integrated Eq. (4.2) or (4.7) to describe the expansion.

B. Astrophysical systems

We turn now to a discussion of macroscopic systems such as supernovae and neutron stars. Here a hydrodynamic description is more accurate, provided one modifies Eqs. (4.1) and (4.2) to include the gravitational force using general relativity.[22] For simplicity, we will not consider the formation of shocks and the resulting nonequilibrium dynamics. Instead, we focus on the infall of stellar matter before the "bounce" and on the properties of the residual matter and the resulting neutron stars.

The interesting feature here is that the flow of the system is determined primarily by gravity and not the pressure gradients, at least in the early stages of stellar collapse. Thus, the possibility of (essentially) constant local v or P/B becomes relevant. There are two limiting cases determined by the viscosity of the matter, which produces friction between neighboring fluid elements. If the viscosity is high, we expect a homologous flow and a constant ("terminal") velocity. In contrast, if friction is small, there is no transfer of longitudinal momentum between neighboring elements, and the fluid travels along streamlines, with constant P/B.

We must therefore consider the implications of covariance on the thermodynamic parameters. For simplicity, we will consider $T = 0$, but our discussion can be extended to finite temperature by replacing the energy E with the Helmholtz free energy $F = E - TS$. As before, we assume that the local variables can be computed from the results for an infinite system.

To begin, consider the energy/baryon $(E/B - M)$ as a function of the proper baryon density, as shown in Fig. 13. These curves can be interpreted as the energy/baryon seen by different observers as they move with various velocities through the infinite system. It is tempting for each observer to conclude that hydrostatic equilibrium

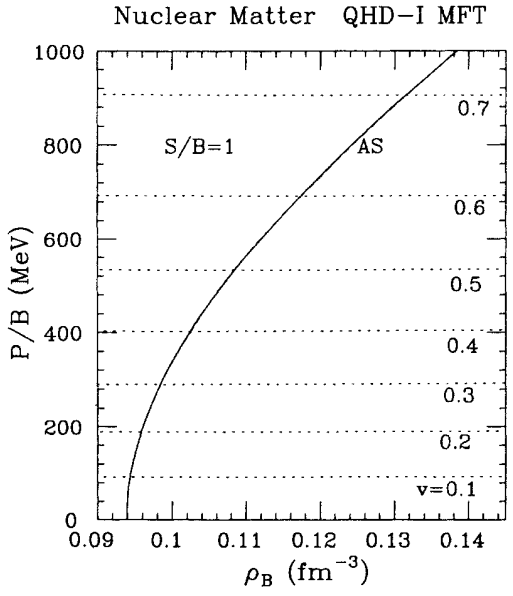

FIG. 12. The adiabatic spinodal (solid) for a moving system with $S/B = 1$ as a function of the laboratory baryon density and local P/B. The dotted curves show the corresponding velocity contours.

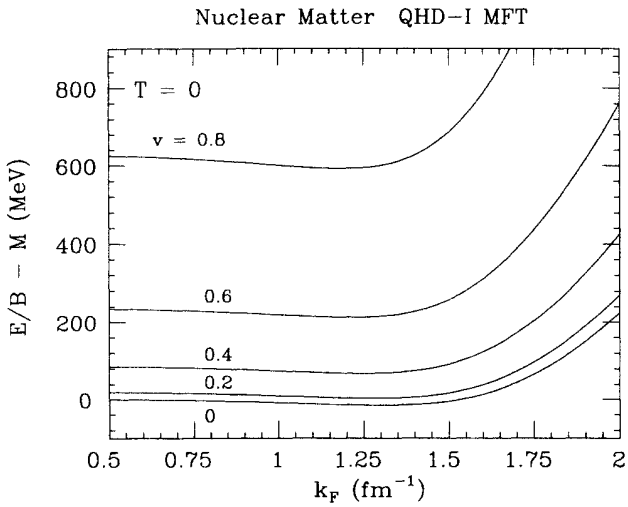

FIG. 13. Laboratory energy/baryon as a function of the proper baryon density ($\rho_{\rm B}' = 2k_{\rm F}^3/3\pi^2$) at zero temperature. The curves are labeled by the velocity of the nuclear fluid relative to the observer.

exists at the minimum in each curve, with a binding energy equal to the value at the minimum. This conclusion is clearly absurd, as it implies that simply by moving through the medium, one observes the matter as unbound! Moreover, it appears that as the observer's velocity increases, the equilibrium proper density $\rho_0 \equiv (\rho_B')_{eq}$ decreases, in direct violation of special relativity!

There are several errors in this naive interpretation.[51] First of all, the binding energy of the system is defined by the energy/baryon in the *comoving* frame, a point that we will return to later. More seriously, although hydrostatic equilibrium occurs when $p=0$, the pressure is not determined by the slopes of the curves in Fig. 13, since the curves are at constant velocity. In other words, since $E=E(V,B,\mathbf{P})$ at zero temperature [see Eq. (3.15)],

$$p \neq -\left[\frac{\partial E}{\partial V}\right]_{B,v} = \rho_B^2 \left[\frac{\partial(\mathcal{E}/\rho_B)}{\partial \rho_B}\right]_v = \eta \frac{k_F}{3} \rho_B' \left[\frac{\partial(\mathcal{E}/\rho_B)}{\partial k_F}\right]_v . \tag{4.9}$$

Thus the points of zero slope in Fig. 13 do not correspond to hydrostatic equilibrium.

In contrast, consider E/B at various values of P/B as seen by a single observer (Fig. 14). The velocity of the system decreases as the density increases along *each* curve; thus, one cannot describe each curve as a boost of the observer, and it is more relevant to plot E/B against the observed (laboratory) baryon density. Since E is a natural function of $\mathbf{P}$, we can determine the pressure from (3.15):

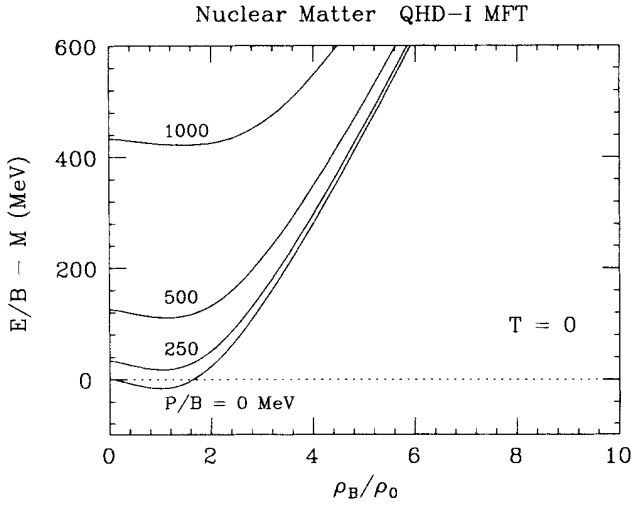

FIG. 14. Laboratory energy/baryon as a function of the laboratory baryon density at zero temperature. The curves are labeled by the momentum/baryon. The equilibrium proper density (ρ_0) sets the density scale.

$$p = -\left[\frac{\partial E}{\partial V}\right]_{B,\mathbf{P}} = -\left[\frac{\partial(E/B)}{\partial(V/B)}\right]_{B,\mathbf{P}/B} = \rho_B^2 \left[\frac{\partial(\mathcal{E}/\rho_B)}{\partial \rho_B}\right]_{\mathbf{P}/B} . \tag{4.10}$$

Here B is held fixed, so we define intensive quantities by dividing everything by B. (In contrast, if V were fixed, we would divide everything by V; see the discussion below.) Thus the minima in Fig. 14 correspond to equilibrium densities, and a careful examination of the curves shows that the observed equilibrium density increases with increasing P/B. Note that all of the equilibrium points correspond to bound systems ($E'/B < M$), when the binding energy is calculated correctly, as we describe later. Moreover, whereas the (incorrect) interpretation of Fig. 13 implies a stiffer system as v increases, the correct results at constant P/B show that the system gets *softer* as the momentum/baryon increases.

To see why the equilibrium density increases as P/B increases, we again consider M_{hyd}, which is given at zero temperature by $M_{hyd}=\eta^2\mu=\eta\mu'$. Evidently, the moving system can achieve the same P/B by decreasing v and increasing M_{hyd}, which occurs at increased ρ_B (see Fig. 11). Although the density increases, the smaller velocity implies a more spherical Fermi surface, which lowers the total energy of the system. Of course, if the density is increased too much, E/B increases in spite of the more spherical Fermi surface. Nevertheless, a slight increase in the density leads to a lower E/B and causes the minima of the curves in Fig. 14 to shift to higher density as P/B increases.

As an aside, note that since V is not held fixed, we cannot define the intensive variables in Eq. (4.10) by dividing by V. Thus,

$$p \neq \rho_B^2 \left[\frac{\partial(\mathcal{E}/\rho_B)}{\partial \rho_B}\right]_{\mathcal{P}} , \tag{4.11}$$

and plotting E/B for various $\mathcal{P}=P/V$ (as opposed to P/B) does *not* allow for a determination of hydrostatic equilibrium. Moreover, although we still have

$$\mu \equiv \left[\frac{\partial E}{\partial B}\right]_{V,\mathbf{P}} = \left[\frac{\partial(E/V)}{\partial(B/V)}\right]_{V,\mathbf{P}/V} = \left[\frac{\partial \mathcal{E}}{\partial \rho_B}\right]_{\mathcal{P}} , \tag{4.12}$$

we can no longer combine this result with Eq. (4.10) in a simple way, since different variables are held fixed when performing the derivatives. To be precise, at $T=0$ we find [see Eqs. (3.50) and (4.10)]

$$p = \eta^2 \mu \rho_B - \mathcal{E} = \rho_B^2 \left[\frac{\partial(\mathcal{E}/\rho_B)}{\partial \rho_B}\right]_{\mathbf{P}/B} = \rho_B \left[\frac{\partial \mathcal{E}}{\partial \rho_B}\right]_{\mathbf{P}/B} - \mathcal{E} \neq \mu \rho_B - \mathcal{E} . \tag{4.13}$$

This result implies

$$\left[\frac{\partial \mathcal{E}}{\partial \rho_B}\right]_{\mathbf{P}/B} = \eta^2 \mu = \eta^2 \left[\frac{\partial \mathcal{E}}{\partial \rho_B}\right]_{\mathbf{P}/V} , \tag{4.14}$$

which can be proven directly using Lorentz covariance and the first law of thermodynamics.

To discuss systems at constant velocity correctly, we can construct an "internal" energy U that is a natural function of $\mathbf{v}$ by making a Legendre transformation:

$$U \equiv U(V,B,\mathbf{v}) \equiv E - \mathbf{v}\cdot\mathbf{P} \quad (T=0) \; . \tag{4.15}$$

In Fig. 15, we plot U/B as a function of the proper baryon density (or k_F). Since v is fixed along each curve, we can again interpret these results as the internal energy seen by observers moving through the system at different velocities. The pressure follows from Eq. (4.15) as

$$p = -\left(\frac{\partial U}{\partial V}\right)_{B,\mathbf{v}} = \rho_B^2 \left(\frac{\partial (U/B)}{\partial \rho_B}\right)_{\mathbf{v}} = \eta \frac{k_F}{3} \rho_B' \left(\frac{\partial (U/B)}{\partial k_F}\right)_{\mathbf{v}} , \tag{4.16}$$

so the minima in these curves correspond to hydrostatic equilibrium. Each observer now finds the same proper equilibrium density ρ_0, in agreement with special relativity.

The shapes of the curves in Fig. 15 are not identical, however, due to the overall factor of η in Eq. (4.16). If we consider instead the Lorentz scalar quantity

$$\frac{\eta U}{B} = \frac{\eta (E - \mathbf{v}\cdot\mathbf{P})}{B} = \frac{\mathcal{E}'}{\rho_B'} \tag{4.17}$$

and remember that $\mathbf{v}$ is fixed in Eq. (4.16), we can rewrite that equation as

$$p = \frac{1}{\eta} \rho_B^2 \left(\frac{\partial (\eta U/B)}{\partial \rho_B}\right)_{\mathbf{v}} = (\rho_B')^2 \left(\frac{\partial (\mathcal{E}'/\rho_B')}{\partial \rho_B'}\right) , \tag{4.18}$$

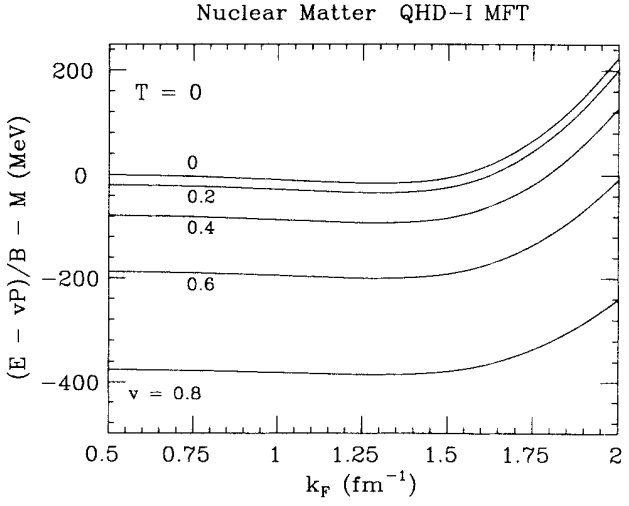

FIG. 15. Internal energy/baryon in the laboratory as a function of the proper baryon density at zero temperature. The curves are labeled by the velocity of the nuclear fluid relative to the observer.

which is the familiar result for p expressed in terms of proper quantities [see Eq. (2.24)].

It now follows that by adding M to the curves in Fig. 15 and multiplying each one by the appropriate $\eta = (1-v^2)^{-1/2}$, we arrive at a single universal curve, equal to $\mathcal{E}'/\rho_B'$. This is just the proper energy/baryon, which defines the binding energy. Thus observers with different velocities agree on both the proper equilibrium density and the binding energy. Similar manipulations with the results in Fig. 14 reveal that at fixed P/B, although the equilibrium density increases substantially as P/B increases, the binding energies of the equilibrium systems remain remarkably constant, and all the equilibrium systems are bound.

In summary, although much of this discussion deals with simple thermodynamics, it emphasizes the care required to interpret results calculated in different frames. In the present case, the incorrect interpretations produce obvious nonsense; in more sophisticated circumstances, however, the errors may not be so obvious.

V. SUMMARY

In this paper we studied the properties of hot, dense, flowing nuclear matter. Since the system is inherently relativistic, we used quantum field theory based on a local, Lorentz-invariant Lagrangian density to describe the dynamics. We discussed some general features of covariant thermodynamics and illustrated these features in an explicit mean-field model. We verified that our approximate microscopic calculation satisfies Lorentz covariance and the appropriate thermodynamic identities. It is important to maintain these identities in more sophisticated calculations, and it is useful, if not essential, to perform these calculations in a covariant fashion.

One of the interesting features of our covariant microscopic approach is the elevation of the velocity $\mathbf{v}$ and momentum density $\mathcal{P}$ to the status of conjugate thermodynamic parameters for the moving system. This is relevant for studying the properties of dense, rapidly flowing matter, and in standard microscopic approaches, the connection of $\mathbf{v}$ and $\mathcal{P}$ to the thermodynamic state functions is usually overlooked. Using a simple hydrodynamic model to consider heavy-ion collisions and astrophysical systems, we illustrated how these new thermodynamic parameters enter and stressed their importance when using thermodynamic identities and differential relations in different reference frames. We expect that the general features discussed here will remain valid in more sophisticated calculations, which are currently under investigation.

ACKNOWLEDGMENTS

We thank C. J. Horowitz and J. D. Walecka for useful discussions. This work was supported in part by Department of Energy Contracts DE-AC05-84ER40150, DE-FG02-87ER40365, and DE-FG05-87ER40322.

*Permanent address: Physics Department and Nuclear Theory Center, Indiana University, Bloomington, Indiana 47405.
[1]E. V. Shuryak, Phys. Rep. **61**, 71 (1980).
[2]H. A. Weldon, Phys. Rev. D **26**, 1394 (1982); **28**, 2007 (1983).
[3]E. V. Shuryak, Phys. Rep. **115**, 151 (1984).
[4]H. Satz, Annu. Rev. Nucl. Part. Sci. **35**, 245 (1985).
[5]L. Dolan and R. Jackiw, Phys. Rev. D **9**, 3320 (1974).
[6]S. Weinberg, Phys. Rev. D **9**, 3357 (1974).
[7]M. B. Kislinger and P. D. Morley, Phys. Rev. D **13**, 2765 (1976); **13**, 2771 (1976).
[8]P. D. Morley and M. B. Kislinger, Phys. Rep. **51**, 63 (1979).
[9]H. A. Bethe, Annu. Rev. Nucl. Part. Sci. **38**, 1 (1988).
[10]B. D. Serot and J. D. Walecka, Adv. Nucl. Phys. **16**, 1 (1986).
[11]G. Baym and L. P. Kadanoff, Phys. Rev. **124**, 287 (1961).
[12]G. Baym, Phys. Rev. **127**, 1391 (1962).
[13]J. D. Walecka, Ann. Phys. (N.Y.) **83**, 491 (1974).
[14]N. P. Landsman and Ch. G. van Weert, Phys. Rep. **145**, 141 (1987).
[15]E. Dagotto, A. Moreau, and U. Wolff, Phys. Rev. Lett. **57**, 1292 (1986).
[16]F. Karsch, Nucl. Phys. **A461**, 305c (1987).
[17]R. J. Furnstahl, R. J. Perry, and B. D. Serot, Phys. Rev. C **40**, 321 (1989).
[18]H. Uechi, Ph.D. thesis, Indiana University, 1988.
[19]R. C. Tolman, *Relativity, Thermodynamics, and Cosmology* (Oxford University Press, Oxford, 1946).
[20]W. Israel, Ann. Phys. (N.Y.) **100**, 310 (1976); Physica **106A**, 204 (1981).
[21]R. A. Freedman, Ph.D. thesis, Stanford University, 1978.
[22]C. W. Misner, K. S. Thorne, and J. A. Wheeler, *Gravitation* (Freeman, San Francisco, 1973).
[23]I. Ojima, Lett. Math. Phys. **11**, 33 (1986).
[24]D. Schütte, Z. Phys. A **326**, 383 (1987).
[25]R. J. Furnstahl and B. D. Serot (unpublished).
[26]A. L. Fetter and J. D. Walecka, *Quantum Theory of Many-Particle Systems* (McGraw-Hill, New York, 1971).
[27]A. L. Fetter and J. D. Walecka, *Theoretical Mechanics of Particles and Continua* (McGraw-Hill, New York, 1980).
[28]J. D. Walecka, in *New Vistas in Nuclear Dynamics,* edited by P. J. Brussaard and J. H. Koch (Plenum, New York, 1986), p. 229.
[29]A. F. Bielajew, Ph.D. thesis, Stanford University, 1982.
[30]R. J. Furnstahl and B. D. Serot, Nucl. Phys. **A468**, 539 (1987).
[31]Some of these results were presented previously at a workshop. See B. D. Serot, in *Relativistic Nuclear Many-Body Physics,* edited by B. C. Clark, R. J. Perry, and J. P. Vary (World Scientific, Singapore, 1989), p. 234.
[32]J. D. Bjorken and S. D. Drell, *Relativistic Quantum Fields* (McGraw-Hill, New York, 1965).
[33]C. Itzykson and J. B. Zuber, *Quantum Field Theory* (McGraw-Hill, New York, 1980).
[34]Equation (3.11) corrects a misprint in Eq. (3.82) of Ref. 10.
[35]This definition of the entropy agrees with $S=-\mathrm{Tr}(\hat{\rho}\ln\hat{\rho})$, where $\hat{\rho}$ is the statistical density operator.
[36]Note that even at low temperatures, there are still solutions with $E^*(\kappa)-\mathbf{v}\cdot\boldsymbol{\kappa}-\nu>0$ for all $\boldsymbol{\kappa}$, corresponding to a dilute classical gas.
[37]J. M. Eisenberg and W. Greiner, *Nuclear Models* (North-Holland, Amsterdam, 1987), Sec. 17.1.
[38]C. J. Horowitz and B. D. Serot, Nucl. Phys. **A368**, 503 (1981).
[39]G. Bertsch and P. J. Siemens, Phys. Lett. **126B**, 9 (1983).
[40]D. H. Boal, Nucl. Phys. **A447**, 479c (1985).
[41]B. M. Waldhauser, J. Theis, J. A. Maruhn, H. Stöcker, and W. Greiner, Phys. Rev. C **36**, 1019 (1987).
[42]J. Diaz Alonso, J. M. Ibañez, and H. Sivak, Phys. Rev. C **39**, 671 (1989).
[43]V. J. Pandharipande and D. G. Ravenhall, in *Nuclear Matter and Heavy-Ion Collisions,* Proceedings of the 1989 Les Houches Winter School (Plenum, New York, in press).
[44]R. J. Furnstahl and C. E. Price, Phys. Rev. C **40**, 1398 (1989).
[45]M. Fukugita and A. Ukawa, Phys. Rev. Lett. **57**, 503 (1986).
[46]S. Gottlieb, W. Liu, D. Toussaint, R. L. Renken, and R. L. Sugar, Phys. Rev. D **35**, 3972 (1987).
[47]P. J. Siemens, Nature **305**, 410 (1983).
[48]N. K. Glendenning, L. P. Csernai, and J. I. Kapusta, Phys. Rev. C **33**, 1299 (1986).
[49]G. Bertsch and J. Cugnon, Phys. Rev. C **24**, 2514 (1981).
[50]S. Weinberg, *Gravitation and Cosmology* (Wiley, New York, 1972), Chap. 2.
[51]We remark, however, that graphs like Fig. 13 are sometimes shown in the literature to illustrate the increasing "stiffness" of the nuclear matter as the velocity is increased. For example, see I. Lovas, Nucl. Phys. **A367**, 509 (1981).